TCR signaling via NFATc1 constrains IL-15-induced NK-like activation of human memory CD8$^+$ T cells

Hoyoung Lee[1,2,5], So-Young Kim[1,5], Sang-Hoon Kim[1,2], Seongju Jeong[1], Kyung Hwan Kim[1], Chang Gon Kim[1], June-Young Koh[1], Hyung-Don Kim[1], Ji Won Han[1], Hosun Yu[1], Sunwoo Min[3], Su-Hyung Park[1,*], Hyuk Soo Eun[4,*], Eui-Cheol Shin[1,2,*]

[1]Graduate School of Medical Science and Engineering, Korea Advanced Institute of Science and Technology (KAIST), Daejeon 34141, Republic of Korea

[2]The Center for Viral Immunology, Korea Virus Research Institute, Institute for Basic Science (IBS), Daejeon 34126, Republic of Korea

[3]Department of Biochemistry, College of Natural Sciences, Chungnam National University, Daejeon, 34134, Republic of Korea

[4]Department of Internal Medicine, Chungnam National University School of Medicine, Daejeon 35015, Republic of Korea

[5]These authors contributed equally to this work

***Correspondence to:**

Eui-Cheol Shin, M.D., Ph.D., Laboratory of Immunology and Infectious Diseases, Graduate School of Medical Science and Engineering, KAIST, 291 Daehak-ro, Yuseong-gu, Daejeon 34141, Republic of Korea; Tel. +82-42-350-4236; Fax. +82-42-350-4240; email: ecshin@kaist.ac.kr

Hyuk Soo Eun, M.D., Ph.D., Department of Internal Medicine, Chungnam National University School of Medicine, Daejeon 35015, Republic of Korea; Tel. +82-42-280-7418; email: hyuksoo@cnu.ac.kr

Su-Hyung Park, Ph.D., Laboratory of Translational Immunology and Vaccinology, Graduate School of Medical Science and Engineering, KAIST, 291 Daehak-ro, Yuseong-gu, Daejeon 34141, Republic of Korea; Tel. +82-42-350-4288; Fax. +82-42-350-4240; email: park3@kaist.ac.kr

Summary

Here we investigated the regulatory mechanisms of TCR-independent bystander activation and NK-like cytotoxicity of human memory $CD8^+$ T cells. We found that TCR signals suppressed characteristic features of IL-15-induced $CD8^+$ T-cell activation, including increased NKG2D expression and upregulation of genes related to NK cytotoxicity and IFN response. Moreover, ionomycin suppressed IL-15-induced bystander activation and NK-like cytotoxicity, indicating that Ca^{2+}-calcineurin signaling is responsible for TCR-mediated suppression of IL-15-induced bystander activation. In detail, NFATc1 suppressed IL-15-induced bystander activation via binding to AP-1 that is necessary for the IL-15-induced upregulation of NK cytotoxicity-related genes. Consistent with these results, calcineurin inhibitors enhanced IL-15-induced NKG2D expression in the presence of TCR signals. Additionally, we defined genes upregulated by IL-15 and downregulated by concurrent TCR signals as an IL-15-induced bystander activation gene set, and found that this gene signature was upregulated in bystander $CD8^+$ T cells from patients with hepatitis A virus infection. This study paves the way for further investigation of bystander $CD8^+$ T-cell activation in various pathological conditions, and its regulation.

Keywords: Bystander activation, IL-15, TCR, Ca^{2+}-calcineurin signaling, NFATc1

Graphical abstract

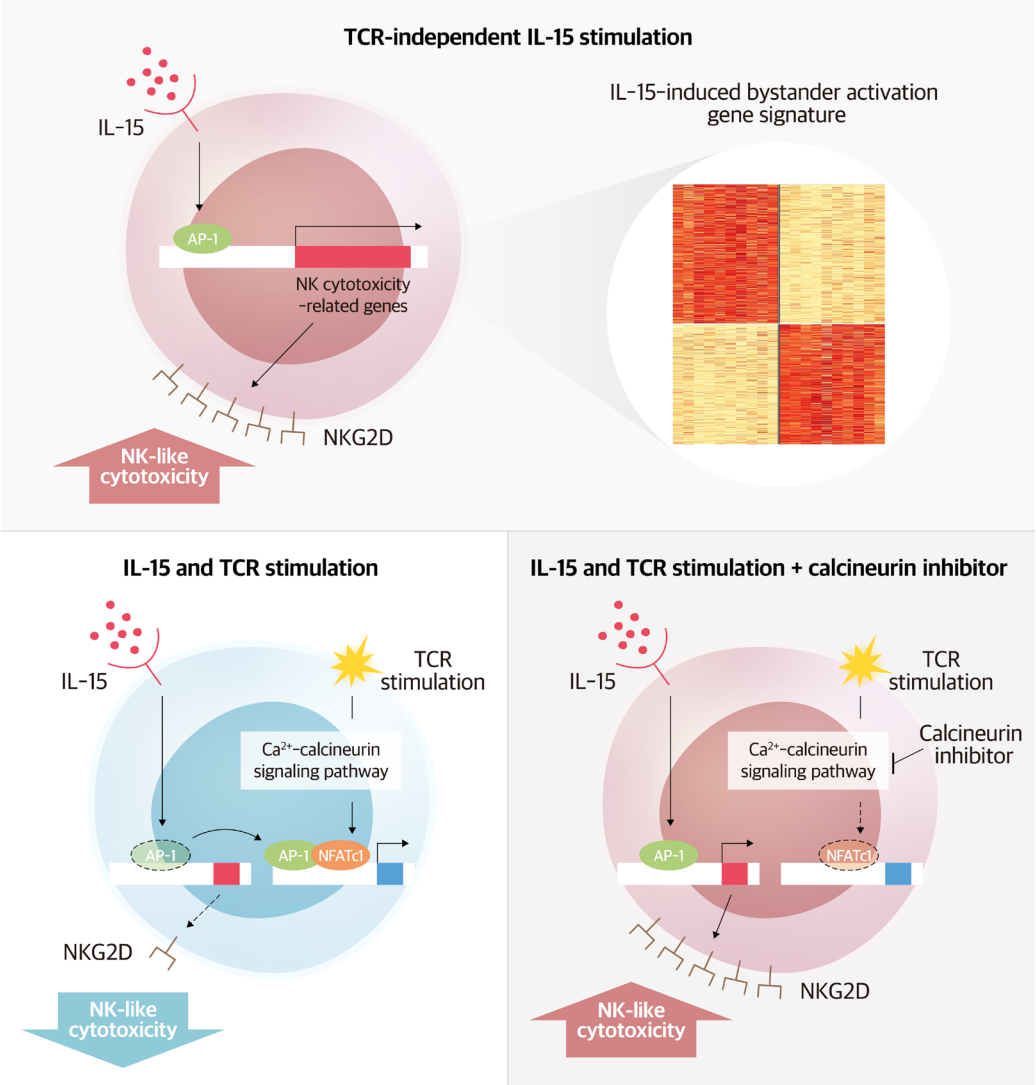

Highlights

- TCR signaling downregulates IL-15-induced transcriptomic features related to NK-like bystander activation of human memory CD8$^+$ T cells via the Ca^{2+}-calcineurin pathway.
- NFATc1 suppresses IL-15-induced bystander activation via binding to AP-1, which is responsible for IL-15-induced NK-like cytotoxic activity.
- Calcineurin inhibitors cannot suppress IL-15-induced bystander CD8$^+$ T-cell activation, and paradoxically increase IL-15-induced NKG2D expression in the presence of TCR signals.
- Genes upregulated by IL-15 and downregulated by concurrent TCR signals define the gene set of bystander CD8$^+$ T-cell activation, which was validated in disease contexts.

61 **Introduction**

62 Memory CD8$^+$ T cells provide prompt and enhanced protection against re-exposures to
63 previously encountered pathogens. These cells are primarily activated by T-cell receptor
64 (TCR) signals, which are triggered by binding to epitope peptides presented by major
65 histocompatibility complex class I (MHC-I).[1] However, memory CD8$^+$ T cells can also be
66 activated without TCR stimulation by cytokines, a process termed bystander activation.[2,3]
67 Interleukin 15 (IL-15) is reportedly the key driver triggering bystander activation of memory
68 CD8$^+$ T cells.[4,5,6,7,8,9,10]

69 Bystander activation of memory CD8$^+$ T cells can play either protective[6,9,11,12,13,14] or
70 detrimental[8,15,16,17,18] roles in microbial infections, depending on the infecting pathogens. For
71 example, in acute hepatitis A virus (HAV) infection, upregulated IL-15 causes bystander
72 activation of pre-existing memory CD8$^+$ T cells that are specific for HAV-unrelated viruses.[8]
73 These bystander-activated memory CD8$^+$ T cells are characterized by increased expression of
74 the NK-activating receptor NKG2D, together with cytotoxic effector molecules, such as
75 perforin and granzyme B. Consequently, the bystander-activated memory CD8$^+$ T cells
76 recognize and kill target cells via NKG2D-dependent NK-like cytotoxicity, leading to non-
77 specific killing of hepatocytes during acute HAV infection. Notably, this IL-15-induced NK-like
78 cytotoxicity is significantly correlated with liver damage severity in patients with acute HAV
79 infection, indicating the immunopathological role of IL-15-driven bystander-activated
80 memory CD8$^+$ T cells.[8]

81 IL-15-induced bystander-activated memory CD8$^+$ T cells are characterized by
82 upregulated NKG2D and CCR5, which is counteracted by the concurrent TCR stimulation.[8,19]
83 Thus, we can distinguish *bona fide* TCR-independent bystander activation from TCR-
84 mediated conventional activation by examining the expression levels of NKG2D[8] and CCR5[19]
85 on CD8$^+$ T cells. Additionally, studies of a mouse model of bystander activation revealed that
86 IL-15-induced upregulation of IFN-induced transmembrane protein 3 (IFITM3) is also
87 counteracted by concurrent TCR stimulation.[20] These findings indicate that antigen-specific
88 TCR signals restrain cytokine-driven nonspecific activation of memory CD8$^+$ T cells. However,
89 the regulatory mechanisms of IL-15-induced bystander activation of memory CD8$^+$ T cells
90 have not yet been investigated at the molecular level.

91 In the present study, we investigated specific transcriptional features and regulatory
92 mechanisms of IL-15-induced bystander $CD8^+$ T-cell activation. We identified a unique set of
93 genes that were upregulated by IL-15 and downregulated by concurrent TCR stimulation.
94 This gene signature, which is related to NK-cell-mediated cytotoxicity and IFN response, was
95 significantly enriched in bystander $CD8^+$ T cells from patients with acute HAV infection. We
96 demonstrated that TCR-induced Ca^{2+}-calcineurin signaling counteracted IL-15-induced
97 bystander activation and NK-like cytotoxic activity. Particularly, NFATc1 suppressed IL-15-
98 induced bystander activation via AP-1 binding. Accordingly, calcineurin inhibitors increased
99 IL-15-induced NKG2D upregulation in the presence of TCR signaling. The current findings
100 reveal a regulatory mechanism of bystander $CD8^+$ T-cell activation, and provide a bystander
101 activation-specific gene signature that will be useful for further investigations of bystander
102 $CD8^+$ T-cell activation in various human diseases.

Results

TCR stimulation counteracts IL-15-induced NKG2D upregulation on memory CD8$^+$ T cells

We analyzed the expression of NKG2D, a marker that is upregulated upon bystander activation[8], on human CD8$^+$ T cells following *ex vivo* stimulation of healthy donor peripheral blood mononuclear cells (PBMCs) with common gamma chain cytokines, including IL-2, IL-4, IL-7, IL-9, IL-15, and IL-21. The NKG2D expression on CCR7$^-$ memory CD8$^+$ T cells was increased by IL-2, but was more significantly upregulated by IL-15 (**Figure 1A**). On the other hand, any of the tested cytokines did not increase NKG2D expression in naïve CD8$^+$ T cells (**Figure S1**). This IL-15-mediated increase in NKG2D expression on memory CD8$^+$ T cells was dose-dependent, and the effect was saturated at 10 ng/ml (**Figure 1B**).

Next, we examined how TCR stimulation affected NKG2D expression on memory CD8$^+$ T cells. From healthy donor PBMCs, we sorted CCR7$^-$ memory CD8$^+$ T cells to a purity above 99% (**Figure S2**). Following treatment with IL-15, anti-CD3, or both, the NKG2D expression on memory CD8$^+$ T cells was significantly upregulated by IL-15 but not by anti-CD3, and was rather restrained by concurrent anti-CD3 stimulation (**Figure 1C**), confirming our previous findings.[8] In addition, we found mRNA expression of *HCST*, which encodes DAP10, an adaptor molecule for NKG2D, exhibited the same pattern as surface NKG2D expression on memory CD8$^+$ T cells in response to IL-15, anti-CD3, or both (**Figure 1D**). This aligns with previous findings in NK cells, where surface NKG2D expression was shown to correlate with *HCST* (DAP10) mRNA levels following IL-15 stimulaiton.[21]

On the other hand, memory CD8$^+$ T-cell activation—as indicated by increased co-expression of CD38 and HLA-DR—was synergistically increased by co-stimulation with IL-15 and anti-CD3, compared to by their individual treatment (**Figure 1E**). Upon co-treatment with IL-15 and anti-CD3, memory CD8$^+$ T cells also exhibited synergized increases of Ki-67 expression (**Figure 1F**) and actual proliferation (**Figure 1G**). Taken together, our results demonstrated that TCR and IL-15 synergistically activate memory CD8$^+$ T cells while certain aspects of IL-15-induced bystander activation (e.g., NKG2D upregulation) is suppressed by TCR stimulation.

TCR stimulation suppresses the IL-15-induced upregulation of genes associated with NK-

133 **cell-mediated cytotoxicity and IFN response in memory CD8$^+$ T cells**

134 To investigate distinct transcriptional signatures induced by IL-15 and TCR stimulation, we
135 performed bulk RNA-seq of sorted memory CD8$^+$ T cells following stimulation with IL-15,
136 anti-CD3, or the combination of both. Principal component analysis (PCA) revealed clear
137 segregation of IL-15-stimulated memory CD8$^+$ T cells from memory CD8$^+$ T cells stimulated
138 with anti-CD3 or the combination of IL-15 and anti-CD3 (**Figure 2A**). This indicated that IL-15-
139 stimulated memory CD8$^+$ T cells exhibited unique transcriptional features compared to the
140 others. We identified upregulated differentially expressed genes (DEGs) (**Figure 2B**) and
141 clustered them according to their upregulation patterns (clusters 1–7) (**Figure 2C and Table**
142 **S1**). Among the 1,401 DEGs upregulated by IL-15 stimulation, 1,037 were additively or
143 synergistically upregulated by IL-15 and anti-CD3 co-stimulation (Cluster 7) indicating
144 additive/synergistic interaction between TCR- and IL-15-induced signals. On the other hand,
145 we found 118 DEGs were upregulated by IL-15 and not further regulated by concurrent anti-
146 CD3 stimulation (Cluster 6), and 214 were upregulated by IL-15 and downregulated by
147 concurrent anti-CD3 stimulation (Cluster 4).

148 We further directly compared data between IL-15 stimulation and IL-15 plus anti-
149 CD3 co-stimulation (**Figure 2D and Table S2**). We identified a gene set that was upregulated
150 by IL-15 and downregulated by concurrent anti-CD3 (designated as the IL-15-specific gene
151 set), and a gene set that was upregulated by IL-15 and anti-CD3 co-stimulation, but not by IL-
152 15 alone (designated as the TCR-specific gene set). The IL-15-specific gene set included IFN-
153 responsive genes (*IFITM1*, *IFITM2*, *IFITM3*, *PIM1* and *SAMHD1*) and genes associated with
154 NK-cell-mediated cytotoxicity (*HCST*, *NCR3*, *GZMA, CD244 and TYROBP*). The TCR-specific
155 gene set included genes upregulated by TCR stimulation (*IL2RA*, *IFNG*, *NR4A1*, *NR4A2*,
156 *NR4A3*, *IRF4*, *BATF* and *MYC*). Pathway analysis confirmed that the IL-15-specific gene set
157 was significantly enriched with genes related to IFN response and NK-cell-mediated
158 cytotoxicity (**Figure 2E**), and that the TCR-specific gene set was significantly enriched with
159 genes associated with calcineurin-regulated NFAT-dependent transcription, MYC pathway,
160 and cell cycle (**Figure 2F**). Gene set enrichment analysis also demonstrated that the IL-15-
161 specific gene set was significantly enriched with genes associated with the IFN-mediated
162 signaling pathway (**Figure 2G**) and NK-cell-mediated cytotoxicity (**Figure 2H**). Importantly,

163 the IL-15-specific gene set included genes for DAP10 (*HCST*), CCR5 (*CCR5*), and IFITM3
164 (*IFITM3*), which have been shown to be upregulated by IL-15, but downregulated by
165 concurrent TCR stimulation in memory $CD8^+$ T cells.[19,20]
166
167 **Ca^{2+}-mediated signaling suppresses characteristic features of IL-15-induced bystander $CD8^+$**
168 **T-cell activation**
169 We further examined why TCR stimulation suppresses characteristic features of IL-15-
170 induced bystander $CD8^+$ T-cell activation, including the upregulation of genes associated
171 with NK-cell-mediated cytotoxicity and IFN response. We hypothesized that the Ca^{2+}-
172 calcineurin signaling pathway might be responsible for this unique phenomenon, because
173 this pathway is activated by TCR stimulation,[22] but not by IL-15 stimulation. We first
174 confirmed that the calcineurin inhibitor FK506 abrogated the TCR-induced activation and
175 proliferation of memory $CD8^+$ T cells (**Figure S3A**), but not IL-15-induced activation and
176 proliferation (**Figure S3B**). On the other hand, the mTOR inhibitor everolimus abolished both
177 TCR- and IL-15-induced activation and proliferation. Consistent with these findings,
178 treatment with another type of calcineurin inhibitor, cyclosporin A (CsA), significantly
179 abrogated the TCR-induced activation and proliferation of memory $CD8^+$ T cells (**Figure S3C**)
180 but did not observably affect IL-15-induced activation and proliferation (**Figure S3D**).
181 To investigate how the Ca^{2+}-calcineurin signaling pathway influenced IL-15-induced
182 bystander $CD8^+$ T-cell activation, we used the Ca^{2+} ionophore ionomycin.[23] Sorted human
183 memory $CD8^+$ T cells were treated with IL-15, ionomycin, or the combination of both, and
184 then subjected to bulk RNA-seq. PCA revealed clear segregation of IL-15-stimulated memory
185 $CD8^+$ T cells from the memory $CD8^+$ T cells stimulated with ionomycin or a combination of IL-
186 15 plus ionomycin (**Figure 3A**)**.** We identified upregulated DEGs (**Figure 3B**) and clustered
187 them according to their upregulation patterns, from cluster 1 to 7 (**Figure 3C and Table S3**).
188 Like TCR co-stimulation, concurrent ionomycin co-stimulation downregulated a subset of
189 DEGs that were upregulated by IL-15 stimulation (cluster 4). We directly compared IL-15
190 stimulation and co-stimulation with IL-15 plus ionomycin. This led to identification of a gene
191 set that was upregulated by IL-15 and downregulated by concurrent ionomycin treatment
192 (**Figure 3D and Table S4**), which was significantly enriched with genes related to IFN

193 response and NK-cell-mediated cytotoxicity (**Figure 3E**).

194

195 **Ca^{2+}-mediated signaling suppresses IL-15-induced NK-like cytotoxic activity of memory**
196 **$CD8^+$ T cells**

197 We examined the effects of Ca^{2+}-mediated signals on the IL-15-induced NK-like cytotoxic
198 activity of memory $CD8^+$ T cells, which is mediated by IL-15-induced upregulation of NKG2D.[8]
199 First, we analyzed NKG2D expression on sorted memory $CD8^+$ T cells from healthy donors
200 following *ex vivo* stimulation with IL-15, ionomycin, or the combination of both. In line with
201 how TCR stimulation affected IL-15-induced NKG2D expression, ionomycin inhibited IL-15-
202 induced expression of NKG2D on memory $CD8^+$ T cells (**Figure 4A**). However, such
203 ionomycin-induced inhibition did not affect upregulation of the activation markers CD38 and
204 HLA-DR (**Figure 4B**). These findings indicated that Ca^{2+}-mediated signals counteracted only
205 certain aspects of IL-15-induced bystander $CD8^+$ T-cell activation, including the increased
206 surface expression of NKG2D, and the upregulation of genes associated with NK-cell-
207 mediated cytotoxicity and IFN response. We further examined the effect of calcineurin
208 inhibitors on NKG2D expression. As expected, FK506 did not abrogate IL-15-induced NKG2D
209 upregulation on memory $CD8^+$ T cells (**Figure S4**). However, FK506 increased the NKG2D
210 expression when memory $CD8^+$ T cells were stimulated with IL-15 in the presence of anti-
211 CD3 (**Figure 4C**). This observation was consistent with the results of CsA treatment (**Figure**
212 **S5**). This paradoxical effect of calcineurin inhibitors can be explained by inhibition of the
213 counteracting effect of the Ca^{2+}-calcineurin pathway on IL-15-induced NKG2D upregulation.

214 We extended our analysis to examine $CD8^+$ T cells obtained from patients with acute
215 HAV infection, in which the bystander activation of memory $CD8^+$ T cells is well-exemplified.[8]
216 Analyzing the NKG2D expression after one day of *ex vivo* stimulation with IL-15, with or
217 without ionomycin, revealed that IL-15-induced NKG2D upregulation on memory $CD8^+$ T
218 cells was significantly inhibited by the concurrent ionomycin stimulation (**Figure 4D**). We
219 found the same result when we analyzed human cytomegalovirus (HCMV)- and Epstein-Barr
220 virus (EBV)-specific MHC-I multimer$^+$$CD8^+$ T cells. The paradoxical effect of FK506 on NKG2D
221 expression was also observed when memory $CD8^+$ T cells from patients with acute HAV
222 infection were treated with IL-15 in the presence of anti-CD3 (**Figure 4E**). Finally, we

223 investigated the effect of ionomycin on IL-15-induced NK-like cytotoxic activity, which is
224 mediated by NKG2D. We sorted $CD8^+$ T cells from PBMCs of patients with acute HAV
225 infection (**Figure S6**), and evaluated the NK-like cytotoxic activity against K562 target cells
226 that lacked MHC-I expression. We found that ionomycin significantly decreased the IL-15-
227 induced NK-like cytotoxic activity of $CD8^+$ T cells from patients with acute HAV infection
228 (**Figure 4F**). Collectively, our findings demonstrated that the IL-15-induced NK-like cytotoxic
229 activity of bystander-activated memory $CD8^+$ T cells was restrained by the Ca^{2+}-calcineurin
230 signaling pathway.
231
232 **NFATc1 suppresses IL-15-induced NKG2D upregulation via AP-1 binding**
233 We further investigated a mechanism how the Ca^{2+}-calcineurin signaling pathway constrains
234 IL-15-induced NK-like activation of memory $CD8^+$ T cells at the transcription factor level.
235 First, we found that SP600125, a JNK inhibitor, abrogated IL-15-induced NKG2D upregulation
236 (**Figure 5A**). In addition, SR11302, an AP-1 inhibitor, also abolished IL-15-induced NKG2D
237 upregulation, indicating that IL-15 upregulates NKG2D expression via AP-1 (**Figure 5B**).
238 Furthermore, we performed siRNA transfection for knocking-down the expression of c-Jun
239 and c-Fos, and IL-15-induced NKG2D upregulation was successfully abrogated by
240 transfection of siRNAs for c-Jun and c-Fos (**Figure 5C**).
241 Next, we hypothesized that IL-15-induced AP-1 cannot upregulate NKG2D when it is
242 bound by NFATc1 activated by the Ca^{2+}-calcineurin signaling pathway in the presence of
243 concurrent TCR stimulation. To validate this hypothesis, we performed transfection with
244 plasmids coding for wild-type NFATc1 as well as T551A mutant NFATc1 that cannot bind to
245 AP-1.[24] NKG2D was upregulated by IL-15 in memory $CD8^+$ T cells transfected with control
246 plasmids, and wild-type NFATc1 transfection abrogated IL-15-induced NKG2D upregulation
247 (**Figure 5D**). Importantly, the NKG2D expression in T551A NFATc1-transfected cells was
248 significantly higher than that in wild-type NFATc1-transfected cells although it was not fully
249 restored to the level in control plasmid-transfected cells. This result supports our hypothesis
250 that TCR-induced NFATc1 suppresses IL-15-induced NKG2D upregulation via binding to AP-1.
251 We also investigated whether AP-1 directly binds to its predicted binding sites in genes
252 associated with IL-15-induced bystander activation of memory $CD8^+$ T cells and whether this

253 binding diminishes with concurrent TCR stimulation. Chromatin immunoprecipitation
254 followed by quantitative PCR (ChIP-qPCR) confirmed that AP-1 binding at *HCST*, *IFITM3*, and
255 *CCR5* under IL-15 stimulation, which was significantly reduced by concurrent TCR stimulation
256 (**Figure 5E**).
257 Finally, we validated our hypothesis by using PMA that activates AP-1 via protein
258 kinase C activation. In this experiment, we used PMA and ionomycin instead of IL-15 and TCR
259 stimulation. As expected, The NKG2D expression on memory $CD8^+$ T cells was significantly
260 upregulated by PMA but not by ionomycin, and was restrained by combined treatment with
261 PMA and ionomycin (**Figure 5F**). Taken together, we conclude that TCR signaling via NFATc1
262 constrains IL-15-induced NK-like activation of memory $CD8^+$ T cells.
263
264 **The gene set of IL-15-induced bystander activation is defined and validated**
265 In Figure 2D, the IL-15-specific gene set was identified from genes upregulated by IL-15 and
266 downregulated by concurrent anti-CD3 stimulation, suggesting that the IL-15-specific gene
267 set can be used to distinguish IL-15-induced bystander activation from TCR-induced
268 conventional activation. We investigated whether the IL-15-specific gene set was actually
269 upregulated in TCR-independently IL-15-activated bystander $CD8^+$ T cells in acute HAV
270 infection, where the bystander activation of memory $CD8^+$ T cells is well-exemplified.[8]
271 To this end, we performed scRNA-seq using $CD8^+$ T cells obtained from patients with
272 acute HAV infection or healthy donors. We sorted $CD8^+$ T cells from PBMCs, and stained
273 them with DNA-barcoded MHC-I multimers (dCODE dextramers) to detect $CD8^+$ T cells
274 specific for HAV, HCMV, EBV, and influenza A virus (IAV) (**Figure 6A**). We further sorted
275 dCODE dextramer-positive and -negative cells, and then re-mixed them at a 1:9 ratio. Next,
276 the cells were labeled with antibody-derived tags (ADTs), and scRNA-seq was performed
277 using the Chromium system. In uniform manifold approximation and projection (UMAP)
278 visualization, we successfully detected $dCODE^+$ HAV-specific $CD8^+$ T cells, together with
279 HCMV-, EBV- and IAV-specific $CD8^+$ T cells, which we defined as bystander $CD8^+$ T cells
280 (**Figure 6B**). Compared to those from healthy donors, the bystander $CD8^+$ T cells from
281 patients with acute HAV infection exhibited increased surface protein levels of activation
282 markers including CD38 and HLA-DR, and the genes for cytotoxic molecules *PRF1* and *GZMB*

283 (**Figure 6C**). Moreover, we confirmed the upregulation of NKG2D, CCR5 and *HCST* in
284 bystander CD8$^+$ T cells compared to HAV-specific CD8$^+$ T cells (**Figure 6D**). This validated our
285 previous finding[8, 19] that bystander CD8$^+$ T cells are activated during acute HAV infection.
286 Next, we applied the IL-15-specific gene set (which was upregulated by IL-15 and
287 downregulated by concurrent anti-CD3) in bulk RNA-seq to scRNA-seq analysis. The IL-15-
288 specific gene set was significantly enriched in bystander CD8$^+$ T cells compared to HAV-
289 specific CD8$^+$ T cells from patients with acute HAV infection (**Figures 6E and F**). Additionally,
290 we found that the IL-15-specific gene set was significantly enriched in dCODE$^-$
291 effector/memory CD8$^+$ T cell cluster compared to HAV-specific CD8$^+$ T cells from patients
292 with acute HAV infection (**Figure S7**). This indicated that the dCODE$^-$ effector/memory CD8$^+$
293 T-cell population included a considerable proportion of non-HAV-specific bystander cells. On
294 the other hand, the TCR-specific gene set (a gene set that was upregulated by IL-15 and anti-
295 CD3 co-stimulation, but not by IL-15 alone in Figure 2D) was significantly upregulated in
296 HAV-specific CD8$^+$ T cells compared to bystander CD8$^+$ T cells (**Figure 6G**). These findings
297 suggest that the IL-15-specific gene set and TCR-specific gene set will be useful for
298 discriminating between IL-15-induced bystander activation and TCR-induced conventional
299 activation. We also analyzed a gene set that was upregulated by IL-15 and downregulated by
300 concurrent ionomycin treatment, and found that it was significantly enriched in bystander
301 CD8$^+$ T cells compared to HAV-specific CD8$^+$ T cells (**Figure 6H**), indicating that genes
302 upregulated by IL-15 and counteracted by Ca^{2+} are characteristic features of bystander-
303 activated memory CD8$^+$ T cells during acute HAV infection. Finally, we found that activation
304 markers (**Figure 6I**), expression of NKG2D, CCR5 and *HCST* (**Figure 6J**), and enrichment of the
305 IL-15-specific gene set (**Figure 6K**) in bystander CD8$^+$ T cells were significantly
306 downmodulated during the convalescent phase.
307 Detailed analysis revealed that IFN response-related genes (*IFI44L*, *IFIT3*, *IFITM1*,
308 *IFITM2*, *IFNAR1*, *IFNAR2*, *IFNGR1, PIM1 and SAMHD1*) were significantly enriched in
309 bystander CD8$^+$ T cells compared to HAV-specific CD8$^+$ T cells (**Figure S8A**)**.** Furthermore,
310 surface proteins (**Figure S8B**) and genes (**Figure S8C**) associated with NK-cell-mediated
311 cytotoxicity were also significantly increased on bystander CD8$^+$ T cells compared to HAV-
312 specific CD8$^+$ T cells. On the other hand, compared to bystander CD8$^+$ T cells, HAV-specific

313 CD8$^+$ T cells exhibited upregulation of CD38, HLA-DR, PD-1, LAG-3, TIM-3, and CD39,
314 together with *IFNG, PRF1, GZMB,* and *MKI67* (**Figure S9**).
315 We also validated the IL-15-specific gene set in a mouse model of bystander CD8$^+$ T-
316 cell activation, in which OT-1 bystander memory cells are activated by PR8 IAV infection, with
317 or without SIINFEKL co-stimulation.[20] We identified the upregulated DEGs in OT-1 memory
318 cells during PR8 infection, compared to in those cells during PR8 infection and SIINFEKL co-
319 stimulation, and found that the IL-15-specific gene set was significantly enriched among the
320 DEGs from the PR8 mouse model (**Figure S10)**. On the other hand, the TCR-specific gene set
321 was significantly enriched among the upregulated DEGs in OT-1 memory cells during PR8
322 infection and SIINFEKL co-stimulation, compared to those cells during PR8 infection without
323 SIINFEKL co-stimulation. These findings demonstrate that the IL-15-specific gene set and
324 TCR-specific gene set are good indicators of IL-15-induced bystander activation and TCR-
325 induced conventional activation, respectively. We further conclude that the IL-15-specific
326 gene set, which was upregulated by IL-15 and counteracted by concurrent TCR stimulation,
327 can be used to identify memory CD8$^+$ T cells that are activated by an IL-15-induced
328 bystander mechanism under various conditions.

329 **Discussion**

330 The characteristic features of IL-15-induced bystander activation—including NK-like
331 cytotoxicity and the upregulation of NKG2D and CCR5—are differentially regulated by IL-15
332 and TCR stimulation in memory $CD8^+$ T cells.[2,8,19] However, the molecular characteristics and
333 regulatory mechanisms governing this phenomenon have not been previously explored.
334 Here, we identified a specific set of genes related to NK-cell-mediated cytotoxicity and IFN
335 response, which was upregulated by IL-15 but restrained by concurrent TCR stimulation in
336 memory $CD8^+$ T cells. Moreover, we used ionomycin to demonstrate that Ca^{2+}-calcineurin
337 signaling restrained characteristic features of IL-15-induced bystander activation and NK-like
338 cytotoxicity. Furthermore, we showed that NFATc1 suppressed IL-15-induced bystander
339 activation via AP-1 binding. Consistent with these results, calcineurin inhibitors increased the
340 IL-15-induced NKG2D upregulation on memory $CD8^+$ T cells in the presence of TCR signals.
341 We further defined the genes that were upregulated by IL-15 and suppressed by concurrent
342 TCR stimulation as the gene set of IL-15-induced bystander activation. This gene signature
343 was significantly enriched in bystander $CD8^+$ T cells from patients with acute HAV infection, a
344 prototype disease of bystander $CD8^+$ T-cell activation.

345 IL-15 is a homeostatic cytokine that plays essential roles in the development,
346 proliferation, and maintenance of memory $CD8^+$ T cells.[25,26,27,28,29] However, accumulating
347 evidence has expanded our understanding of IL-15 from a homeostatic cytokine to a potent
348 inducer of bystander $CD8^+$ T-cell activation.[2] Previous studies have shown that IL-15 itself
349 elicits multiple functions of memory $CD8^+$ T cells, independently of TCR signals, including
350 proliferation, synthesis of effector molecules, and cytotoxicity.[30,31,32] It was later
351 demonstrated that IL-15 can activate bystander $CD8^+$ T cells and enhance their NK-like
352 cytotoxic features that contribute to host tissue damage.[8,18] However, limited information is
353 available regarding the specific transcriptional signatures induced by bystander activation in
354 memory $CD8^+$ T cells, which are distinguished from those induced by TCR stimulation.
355 Notably, the specific transcriptional profile of IL-15-induced bystander activation has not
356 been previously profiled in human memory $CD8^+$ T cells.

357 In the present study, we found a unique set of genes upregulated by IL-15 and
358 downregulated by concurrent TCR stimulation, which were enriched with genes associated

359 with NK-cell-mediated cytotoxicity and IFN response. This finding supports previous reports
360 of NK-like cytotoxic activity of IL-15-activated memory CD8$^+$ T cells.[5,8,10,31,33,34] Moreover, the
361 enrichment of IFN response genes among genes upregulated by IL-15 and downregulated by
362 concurrent TCR stimulation also confirms our previous findings that IFN response genes
363 were enriched in bystander-activated memory CD8$^+$ T cells from a mouse model.[20] The gene
364 set of IL-15-induced bystander activation, which was upregulated by IL-15 and counteracted
365 by concurrent TCR stimulation, can be used to identify memory CD8$^+$ T cells that are
366 activated by an IL-15-induced bystander mechanism under various conditions.
367 To validate the IL-15-induced bystander activation gene set in a human disease
368 setting, we performed a scRNA-seq analysis that incorporated dCODE MHC-I multimers.
369 Using this approach, we analyzed single-cell transcriptomes of HAV-specific and bystander
370 (HCMV-, EBV-, and IAV-specific) CD8$^+$ T cells from PBMCs of patients with acute HAV
371 infection. Importantly, the IL-15-induced bystander activation gene set that was upregulated
372 by TCR-independent IL-15 stimulation was significantly enriched in bystander CD8$^+$ T cells
373 from these patients. However, this enrichment was not observed in HAV-specific CD8$^+$ T cells
374 during acute HAV infection. This finding demonstrates that gene set will be useful for
375 distinguishing IL-15-induced bystander CD8$^+$ T-cell activation from TCR-mediated
376 conventional activation. This validated IL-15-induced bystander activation gene set provides
377 a compelling opportunity to explore its use in various other diseases with elevated IL-15
378 levels that correlate with disease severity, in which the phenomenon of TCR-independent
379 CD8$^+$ T-cell activation is implicated.[2,35] For example, the IL-15-induced bystander activation
380 gene set could be used to study alopecia areata,[33] in which virtual memory CD8$^+$ T cells
381 activated by IL-15 exert NKG2D-dependent NK-like cytotoxicity. Identifying and analyzing
382 TCR-independent bystander CD8$^+$ T-cell activation in other diseases could enhance our
383 understanding of the roles of bystander-activated CD8$^+$ T cells, elucidating their potential
384 contribution to shaping disease outcomes. Moreover, future research could uncover
385 potential therapeutic targets, which could be used to modulate the immunopathological role
386 of TCR-independent bystander CD8$^+$ T-cell activation in various diseases.
387 Binding of IL-15 to its cellular receptor delivers intracellular signals,[36,37] some of
388 which (e.g., mTOR and MAPK signaling pathways) overlap with those induced by TCR

389 stimulation.[38] Due to the overlapping components of signaling pathways, previous reports
390 have focused on the role of IL-15 in amplifying TCR signaling, thereby enhancing various TCR-
391 mediated effector functions of $CD8^+$ T cells.[39,40,41] However, the Ca^{2+}-calcineurin signaling
392 pathway discriminates between TCR and IL-15 signals. Upon TCR ligation, Ca^{2+} is released
393 into the cytosol, leading to a rapid influx of extracellular Ca^{2+} until its level is highly
394 sustainable for T-cell activation.[42] The accumulated cytosolic Ca^{2+} binds to calmodulin,
395 leading to a subsequent conformational change in calmodulin for its interaction with the
396 protein phosphatase calcineurin.[43] This interaction dephosphorylates NFATc1, which leads to
397 its translocation into the nucleus, where it binds to AP-1 and regulates various T-cell
398 functions.[44, 45] However, IL-15 stimulation does not activate the Ca^{2+}-calcineurin signaling
399 pathway, as indicated by our present finding that calcineurin inhibitors had no effect on IL-
400 15-induced $CD8^+$ T-cell activation. Instead, Ca^{2+} signals suppress characteristic features of the
401 IL-15-induced bystander activation of memory $CD8^+$ T cells, including upregulation of NKG2D
402 the IL-15-induced bystander activation gene set, and NK-like cytotoxic activity.
403 AP-1 is a transcription factor induced by diverse immune signaling pathways,
404 including IL-15.[36] It typically exists as a dimeric complex comprising proteins from the JUN,
405 FOS, ATF, and MAF families.[46] Notably, c-JUN and c-FOS are essential for inducing NKG2D
406 expression by upregulating DAP10 expression.[47] In fact, in our study, we demonstrated that
407 IL-15 upregulates *HCST* mRNA expression and NKG2D surface expression on memory $CD8^+$ T
408 cells. Moreover, we found that AP-1 drives the IL-15-induced upregulation of NKG2D on
409 memory $CD8^+$ T cells. Given that NFATc1 binds AP-1 to form a transcriptional complex,[44] we
410 further investigated whether this interaction under concurrent TCR stimulation abrogates
411 the action of AP-1 regarding the IL-15-induced upregulation of NKG2D and other NK-related
412 genes, including *HCST*. Notably, TCR stimulation promotes NFATc1 binding to AP-1, thereby
413 preventing the AP-1-dependent transcription of key genes involved in IL-15-induced NK-like
414 bystander activation. Our findings reveal a crucial regulatory mechanism, in which TCR
415 signaling counteracts cytokine-induced T-cell activation. This discovery offers new insights
416 into the balance between antigen-specific adaptive and cytokine-induced innate-like T-cell
417 activation.

418 Calcineurin inhibitors, such as FK506 and CsA, are widely used as
419 immunosuppressants in organ transplantation settings and for the treatment of
420 autoimmune diseases.[48] However, previous studies have reported that calcineurin inhibitors
421 do not affect the cytokine-induced production of IL-17A and IFN-γ from mouse memory-like
422 $CD4^+$ T cells.[49] Consistently, we demonstrated that calcineurin inhibitors failed to suppress
423 the IL-15-induced activation and proliferation of memory $CD8^+$ T cells. Moreover, calcineurin
424 inhibitors paradoxically upregulated the IL-15-induced NKG2D expression on memory $CD8^+$ T
425 cells in the presence of TCR co-stimulation. This suggests that calcineurin inhibitors may
426 enhance NK-like cytotoxic activity of memory $CD8^+$ T cells, and exacerbate $CD8^+$ T cell-
427 mediated immunopathology in IL-15-associated pathological conditions. The data from our
428 current study suggests that immunosuppressive regimens must be carefully selected for the
429 treatment of chronic inflammatory diseases, depending on the mechanism of $CD8^+$ T-cell
430 activation.
431 The recent recognition that bystander activation of memory $CD8^+$ T cells can
432 potentially impact disease outcomes has attracted great attention. Our present study
433 highlights characteristic features and regulatory mechanisms underlying IL-15-induced
434 bystander activation in human memory $CD8^+$ T cells. We demonstrated that IL-15-induced
435 bystander activation exhibits NK-like qualities, rather than being an inherent aspect of the
436 adaptive immune response. Moreover, we found that TCR stimulation plays a role in
437 preventing such antigen-nonspecific NK-like activation through Ca^{2+}-calcineurin-NFATc1
438 signaling, thereby preserving the intrinsic nature of the adaptive immune response.
439 Increasing our understanding of the mechanisms underlying the IL-15-induced bystander
440 activation of memory $CD8^+$ T cells will have important clinical implications for the
441 appropriate treatment of patients whose tissues are damaged by $CD8^+$ T cell-mediated
442 immunopathogenesis.

Acknowledgement

This work was supported by the Bio&Medical Technology Development Program of the National Research Foundation (NRF) funded by the Korean government (MSIT) (RS-2024-00439160 and RS-2024-00512914) and by the Institute for Basic Science (IBS), Republic of Korea (IBS-R801-D2).

Author contributions

H.L. and E.C.S. designed the study. H.S.E. collected and provided human clinical samples and information. H.L., S.Y.K., S.H.K., and K.H.K. performed the experiments and collected data. H.L., S.Y.K., S.H.K., H.Y., S.J., K.H.K., C.G.K., J.Y.K., H.D.K., J.W.H., S.H.P., and E.C.S were involved in data analysis and interpretation. H.L., S.Y.K., and H.Y. performed statistical analysis. H.L., S.Y.K., and E.C.S. drafted the manuscript with comments from all authors.

Competing interests

The authors have no conflicts of interest.

INCLUSION AND DIVERSITY

We support inclusive, diverse, and equitable conduct of research.

599 **STAR★METHODS**

600 **KEY RESOURCES TABLE**

REAGENT or RESOURCE	SOURCE	IDENTIFIER
Antibodies		
BV510 Anti-human CD3 (clone UCHT1),	BD Biosciences	Cat# 563109 RRID:AB_2732053
BV605 Anti-human CD8 (clone SK1)	BD Biosciences	Cat# 564116 RRID:AB_2869551
BV711 Anti-human Ki-67 (clone B56)	BD Biosciences	Cat# 563755 RRID:AB_2738406
PerCP-Cy5.5 Anti-human CD4 (clone RPA-T4)	BD Biosciences	Cat# 560650 RRID:AB_1727476
AlexaFluor 700 Anti-human CD3 (clone UCHT1)	BD Biosciences	Cat# 557943 RRID:AB_396952
PerCP-Cy5.5 Anti-human CD14 (clone M5E2)	BD Biosciences	Cat# 550787 RRID:AB_393884
PerCP-Cy5.5 Anti-human CD19 (clone H fIB19)	BD Biosciences	Cat# 561295 RRID:AB_10644017
PE Anti-human NKG2D (clone 1D11)	BD Biosciences	Cat# 561815 RRID:AB_10896282
PE-CF594 Anti-human CD14 (clone MPHIP9)	BD Biosciences	Cat# 562335 RRID:AB_11153663
PE-CF594 Anti-human CD19 (clone HIB19)	BD Biosciences	Cat# 562294 RRID:AB_11154408
Pe-Cy7 Anti-human CD45RA (clone HI100)	BD Biosciences	Cat# 560675 RRID:AB_1727498
AlexaFluor 700 Anti-human CD45RA (clone HI100)	BD Biosciences	Cat# 560673 RRID:AB_1727496

APC Anti-human HLA-DR (clone G46-6)	BD Biosciences	Cat# 559866 RRID:AB_398674
BV650 Anti-Human HLA-DR (clone L203)	BD Biosciences	Cat# 752489 RRID:AB_2917482
AlexaFluor 700 Anti-human CD3 (clone UCHT1)	BD Biosciences	Cat# 557943 RRID:AB_396952
AlexaFluor 700 Anti-human CD38 (clone HIT2)	BD Biosciences	Cat# 560676 RRID:AB_1727472
APC-H7 Anti-human CD8 (clone SK1)	BD Biosciences	Cat# 560273 RRID:AB_1645482
FITC Anti-human CD16 (clone B73.1)	BD Biosciences	Cat# 561308 RRID:AB_10644202
BV421 anti-human NKG2D (clone 1D11)	Biolegend	Cat# 320821 RRID:AB_2566510
PerCP/cy5.5 Anti-human CD197 (CCR7) (clone G043H7)	Biolegend	Cat# 353220 RRID:AB_10916121
APC/Cyanine7 Anti-human HLA-DR (clone L243)	Biolegend	Cat# 307618 RRID:AB_493586
TotalSeq™-C0034 anti-human CD3 Antibody (clone UCHT1)	Biolegend	Cat# 300479 RRID: AB_2800723
TotalSeq™-C0045 anti-human CD4 Antibody (clone SK3)	Biolegend	Cat# 344651 RRID:AB_2800921
TotalSeq™-C0046 anti-human CD8 Antibody (clone SK1)	Biolegend	Cat# 344753 RRID:AB_2800922
TotalSeq™-C0047 anti-human CD56 (NCAM) Antibody (clone 5.1H11)	Biolegend	Cat# 362559 RRID:AB_2801002
TotalSeq™-C0051 anti-human CD14 Antibody (clone 63D3)	Biolegend	Cat# 367137 RRID:AB_2810576
TotalSeq™-C0063 anti-human CD45RA Antibody	Biolegend	Cat# 304163

(clone HI100)		RRID:AB_2800764
TotalSeq™-C0083 anti-human CD16 Antibody (clone 3G8)	Biolegend	Cat# 302065 RRID:AB_2800738
TotalSeq™-C0085 anti-human CD25 Antibody (clone BC96)	Biolegend	Cat# 302649 RRID: AB_2800745
TotalSeq™-C0087 anti-human CD45RO Antibody (clone UCHL1)	Biolegend	Cat# 304259 RRID: AB_2800766
TotalSeq™-C0088 anti-human CD279 (PD-1) Antibody (clone EH12.2H7)	Biolegend	Cat# 329963 RRID: AB_2800862
TotalSeq™-C0089 anti-human TIGIT (VSTM3) Antibody (clone A15153G)	Biolegend	Cat# 372729 RRID: AB_2801021
TotalSeq™-C0101 anti-human CD335 (NKp46) Antibody (clone 9 E2)	Biolegend	Cat# 331941 RRID: AB_2800874
TotalSeq™-C0138 anti-human CD5 Antibody (clone UCHT2)	Biolegend	Cat# 300637 RRID: AB_2800726
TotalSeq™-C0139 anti-human TCR γ/δ Antibody (clone B1)	Biolegend	Cat# 331231 RRID: AB_2814199
TotalSeq™-C0140 anti-human CD183 (CXCR3) Antibody (clone G025H7)	Biolegend	Cat# 353747 RRID: AB_2800949
TotalSeq™-C0141 anti-human CD195 (CCR5) Antibody (clone J418F1)	Biolegend	Cat# 359137 RRID: AB_2810570
TotalSeq™-C0145 anti-human CD103 (Integrin αE) Antibody (clone BerACT8)	Biolegend	Cat# 350233 RRID: AB_2800933
TotalSeq™-C0146 anti-human CD69 Antibody (clone FN50)	Biolegend	Cat# 310951 RRID: AB_2800810
TotalSeq™-C0147 anti-human CD62L Antibody (clone DREG-56)	Biolegend	Cat# 304851 RRID: AB_2800770
TotalSeq™-C0148 anti-human CD197 (CCR7) Antibody (clone G043H7)	Biolegend	Cat# 353251 RRID: AB_2800943

TotalSeq™-C0149 anti-human CD161 Antibody (clone HP-3G10)	Biolegend	Cat# 339947 RRID: AB_2810532
TotalSeq™-C0151 anti-human CD152 (CTLA-4) Antibody (clone BNI3)	Biolegend	Cat# 369621 RRID: AB_2801015
TotalSeq™-C0152 anti-human CD223 (LAG-3) Antibody (clone 11C3C65)	Biolegend	Cat# 369335 RRID: AB_2814327
TotalSeq™-C0154 anti-human CD27 Antibody (clone O323)	Biolegend	Cat# 302853 RRID: AB_2800747
TotalSeq™-C0155 anti-human CD107a (LAMP-1) Antibody (clone H4A3)	Biolegend	Cat# 328649 RRID: AB_2800854
TotalSeq™-C0159 anti-human HLA-DR Antibody (clone L243)	Biolegend	Cat# 307663 RRID: AB_2800795
TotalSeq™-C0165 anti-human CD314 (NKG2D) Antibody (clone 1D11)	Biolegend	Cat# 320837 RRID: AB_2800844
TotalSeq™-C0168 anti-human CD57 Recombinant Antibody (clone QA17A04)	Biolegend	Cat# 393321 RRID: AB_2801030
TotalSeq™-C0169 anti-human CD366 (Tim-3) Antibody (clone F38-2E2)	Biolegend	Cat# 345049 RRID: AB_2800925
TotalSeq™-C0170 anti-human CD272 (BTLA) Antibody (clone MIH26)	Biolegend	Cat# 344527 RRID: AB_2800919
TotalSeq™-C0176 anti-human CD39 Antibody (clone A1)	Biolegend	Cat# 328237 RRID: AB_2800853
TotalSeq™-C0179 anti-human CX3CR1 Antibody (clone K0124E1)	Biolegend	Cat# 355705 RRID: AB_2800960
TotalSeq™-C0224 anti-human TCR α/β Antibody (clone IP26)	Biolegend	Cat# 306743 RRID: AB_2800793
TotalSeq™-C0250 anti-mouse/human KLRG1 (MAFA) Antibody (clone 2F1/KLRG1)	Biolegend	Cat# 138433 RRID: AB_2800649
TotalSeq™-C0355 anti-human CD137 (4-1BB)	Biolegend	Cat# 309839

Antibody (clone 4B4-1)		RRID: AB_2800807
TotalSeq™-C0368 anti-human CD226 (DNAM-1) Antibody (clone 11A8)	Biolegend	Cat# 338337 RRID: AB_2800899
TotalSeq™-C0386 anti-human CD28 Antibody (clone CD28.2)	Biolegend	Cat# 302963 RRID: AB_2800751
TotalSeq™-C0389 anti-human CD38 Antibody (clone HIT2)	Biolegend	Cat# 303543 RRID: AB_2800758
TotalSeq™-C0390 anti-human CD127 (IL-7Rα) Antibody (clone A019D5)	Biolegend	Cat# 351356 RRID: AB_2800937
TotalSeq™-C0420 anti-human CD158 (KIR2DL1/S1/S3/S5) Antibody (clone HP-MA4)	Biolegend	Cat# 339517 RRID: AB_2814252
TotalSeq™-C0581 anti-human TCR Vα7.2 Antibody (clone 3C10)	Biolegend	Cat# 351735 RRID: AB_2810556
TotalSeq™-C0584 anti-human TCR Vα24-Jα18 (iNKT cell) Antibody (clone 6B11)	Biolegend	Cat# 342925 RRID: AB_2810529
TotalSeq™-C0592 anti-human CD158b (KIR2DL2/L3, NKAT2) Antibody (clone DX27)	Biolegend	Cat# 312619 RRID: AB_2819944
TotalSeq™-C0599 anti-human CD158e1 (KIR3DL1, NKB1) Antibody (clone DX9)	Biolegend	Cat# 312725 RRID: AB_2814161
TotalSeq™-C0801 anti-human CD337 (NKp30) Antibody (clone P30-15)	Biolegend	Cat# 325219 RRID: AB_2800851
TotalSeq™-C0802 anti-human CD336 (NKp44) Antibody (clone P44-8)	Biolegend	Cat# 325119 RRID: AB_2810484
TotalSeq™-C0804 anti-human CD186 (CXCR6) Antibody (clone K041E5)	Biolegend	Cat# 356023 RRID: AB_2876677
TotalSeq™-C0867 anti-human CD94 Antibody (clone DX22)	Biolegend	Cat# 305523 RRID: AB_2814143
TotalSeq™-C0896 anti-human CD85j (ILT2) Antibody (clone GHI/75)	Biolegend	Cat# 333725 RRID: AB_2814226

TotalSeq™-C1021 anti-human GPR56 Antibody (clone 4C3)	Biolegend	Cat# 391907 RRID: AB_2832737
CD3 monoclonal antibody (clone OKT3) Functional Grade	Invitrogen	Cat# 16-0037-85 RRID: AB_468854
Fluorescein-conjugated Anti-human CCR7 (clone 150503)	R&D Systems	Cat# FAB197F RRID: AB_2259847
Anti-c-Jun antibody [E254] - ChIP Grade	Abcam	Cat# ab32137 RRID: AB_731608
Rabbit Anti-Mouse IgG H&L	Abcam	Cat# ab46540 RRID: AB_2614925
Chemicals, Peptides and Recombinant Proteins		
Brilliant Stain Buffer	BD Biosciences	Cat# 563794
7-AAD	BD Biosciences	Cat# 559925
Recombinant human IL-2 protein	Peprotech	Cat# 200-0
Recombinant human IL-4 protein	Peprotech	Cat# 200-04
Recombinant human IL-7 protein	Peprotech	Cat# 200-07
Recombinant human IL-9 protein	Peprotech	Cat# 200-09
Recombinant human IL-15 protein	Peprotech	Cat# 200-15
Recombinant human IL-21 protein	Peprotech	Cat# 200-21
Dimethyl sulfoxide	Sigma-Aldrich	Cat# R8418
Cyclosporin A	Sigma-Aldrich	Cat# SML1018
PMA	Sigma-Aldrich	Cat# P1585
Ionomycin calcium salt	Sigma-Aldrich	Cat# I3909
SP600125	Sigma-Aldrich	Cat# S5567
Formaldehyde solution	Sigma-Aldrich	Cat# F8775
Tacrolimus (FK506)	Selleckchem	Cat# S5003
Everolimus (RAD001)	Selleckchem	Cat# S1120
SR 11302	R&D Systems	Cat# 2476
Lymphocyte Separation Medium	Corning	Cat# 25-072-CV

Trizol reagent	Invitrogen	Cat# 15596018
To-Pro™-3 iodide	Invitrogen	Cat# T3605
Pierce™ DSG, No-Weigh™ Format	Thermo Fisher	Cat# 20593
Dynabeads™ Protein A for Immunoprecipitation	Thermo Fisher	Cat# 10001D
Critical Commercial Assays		
LIVE/DEAD fixable aqua dead cell stain kit	Invitrogen	Cat# L34957
LIVE/DEAD fixable Red dead cell stain kit	Invitrogen	Cat# L34972
Intracellular fixation & permeabilization buffer set	Invitrogen	Cat# 88-8824-00
Neon™ NxT Electroporation System 100-µL Kit	Invitrogen	Cat# N10025
CellTrace Violet Cell Proliferation Kit	Invitrogen	Cat# C34557
TaqMan™ Gene Expression Assay (FAM) (Gene Symbol: HCST)	Applied Biosystems	Cat# 4351370 Hs0 0367159_m1
TaqMan™ Gene Expression Assay (FAM) (Gene Symbol: B2M)	Applied Biosystems	Cat# 4331182 Hs00187842_m1
TaqMan Gene Expression Master Mix	Applied Biosystems	Cat# 4369016
RNase A, DNase and protease-free	Thermo Fisher	Cat# EN0531
Anti-FITC microbeads	Miltenyi Biotec	Cat# 130-048-701
CD8 MicroBeads, human	Miltenyi Biotec	Cat# 130-045-201
Human $CD8^+$ T cell isolation kit	Miltenyi Biotec	Cat# 130-096-495
Ribospin total RNA purification kit	Geneall	Cat# 130-090-101
cDNA synthesis master mix	LeGene	Cat# 6290-20
Diluent C for general membrane labeling	Sigma-Aldrich	Cat# CGLDIL
PKH26 Red Fluorescent Cell Linker Kit for General Cell Membrane Labeling	Sigma-Aldrich	Cat# PKH26GL
proteinase K	New England Biolabs	Cat# P8107S
Recombinant DNA		
pcDNA3.1_empty	Genescript	N/A

pcDNA3.1_NFATc1_WT	Genescript	N/A
pcDNA3.1_NFATc1_T551_MT	Genescript	N/A
siRNAs		
Silencer™ Select Negative Control No. 1 siRNA	Invitrogen	Cat# 4390844
Silencer™ Select c-Fos siRNA	Invitrogen	Cat# 4392420
Silencer™ Select c-Jun siRNA	Invitrogen	Cat# 4392420
Cell line		
K562	ATCC	Cat# CCL-243
Software and Algorithms		
FlowJo (version 10.7.2)	Tree Star	https://www.flowjo.com/solutions/flowjo/downloads
Prism (version 8.4)	GraphPad	http://www.graphpad.com/scientific-software/prism/
R v.4.1.0	The R foundation	N/A
Cell Ranger	R package	Version 3.1.0
Seurat package	R package	Version 3.2.2
STAR aligner	R package	Version 2.5.1b
DESeq2	R package	Version 1.24.0
ComplexHeatmap	R package	Version 2.15.4
Bowtie2	R package	Version 2.2.9
limma	R package	Version 4.3
fgsea	R package	Version 1.22.0
biomaRt	R package	Version 2.50.0
GSEA	PMID:17644558	http://www.gsea-msigdb.org/gsea/msigdb/index.jsp
enrichR database	Maayanlab	https://maayanlab.c

		loud/Enrichr/
Dextramers		
HLA-A*0201 (NLVPMVATV), APC CMV Dextramer	Immudex	WB2132- APC-150
HLA-A*0201 (GLCTLVAML), APC EBV Dextramer	Immudex	WB2130- APC-150
HLA-A*0201 LLYNCCYHV (HAV) dCODE Dextramer® grade (Gold)	Immudex	dCODELLYNCCYHV - 50T
HLA-A*0201 NLVPMVATV (CMV) dCODE Dextramer® grade (Gold)	Immudex	dCODENLVPMVATV - 50T
HLA-A*0201 GLCTLVAML (EBV) dCODE Dextramer® grade (Gold)	Immudex	dCODEGLCTLVAML - 50T
HLA-A*0201 GILGFVFTL (IAV) dCODE Dextramer® grade (Gold)	Immudex	dCODEGILGFVFTL50 T

RESOURCE AVAILABILITY

Lead contact

Further information and requests for resources and reagents should be directed to and will be fulfilled by the lead contact, Eui-Cheol Shin (ecshin@kaist.ac.kr).

Materials availability

The study did not produce novel, distinctive materials or substances.

Data and code availability

All analyzed sequencing data will be available online. Bioinformatic analyses were performed using open-source software and in-house scripts in R (version 4.1.0), which are available from the corresponding author upon reasonable request.

STUDY PARTICIPANT DETAILS

Human blood samples

Peripheral blood samples were obtained from healthy volunteers from KAIST Clinic Pappalardo Center, who were not taking any immunosuppressive medications. Peripheral blood samples were also collected from patients with acute HAV infection and also during the convalescent phase, who at admission exhibited clinical and laboratory features of acute hepatitis A (AHA), including seropositivity for anti-HAV IgM and/or IgG antibodies. PBMCs

618 were isolated from whole blood by density gradient centrifugation using Lymphocytes
619 Separation Medium (Corning). The isolated PBMCs were cryopreserved in freezing media
620 containing fetal bovine serum (Corning) with 10% dimethyl sulfoxide (Sigma-Aldrich) until
621 their use. This study was conducted in accordance with the principles of the Declaration of
622 Helsinki, and was approved by the institutional review board of each involved institution
623 (KAIST: KH2018-118 and Chungnam National University Hospital: 2019-03-066-025). Each
624 healthy volunteer and patient with HAV infection gave their written informed consent prior
625 to inclusion in the study.
626
627 **METHOD DETAILS**
628 **Cell sorting**
629 $CD8^+$ T cells were negatively isolated from PBMCs of healthy donors and patients with HAV
630 infection using a $CD8^+$ T-cell isolation kit (Miltenyi Biotec), according to the manufacturer's
631 instructions. Isolated $CD8^+$ T cells were stained with FITC-conjugated anti-CCR7 antibody
632 (R&D systems), and then further stained with anti-FITC microbeads (Miltenyi Biotec),
633 following the manufacturer's instructions for negatively isolating $CCR7^-$ memory $CD8^+$ T
634 cells.
635
636 **In vitro stimulation and proliferation assay**
637 PBMCs were cultured in RPMI 1640 medium (Corning) supplemented with 10% fetal bovine
638 serum (Corning) and 1% penicillin/streptomycin (Sigma-Aldrich). PBMCs were cultured for 48
639 hours with IL-2 (10 ng/ml; Peprotech), IL-4 (10 ng/ml; R&D systems), IL-7 (10 ng/ml;
640 Peprotech), IL-9 (10 ng/ml; Peprotech), IL-15 (10 ng/ml; Peprotech), or IL-21 (10 ng/ml;
641 Peprotech), and we examined the NKG2D expression among $CD8^+$ T cells and their naïve and
642 memory subsets. Sorted $CCR7^-$ memory $CD8^+$ T cells were cultured with IL-15 (10 ng/ml),
643 anti-CD3 (coated, 1 μg/ml; Invitrogen), PMA (10 ng/ml; Sigma-Aldrich), ionomycin (500
644 ng/ml; Sigma-Aldrich), or combinations of these additives, for 48 hours followed by analysis
645 of NKG2D and granzyme B expressions, or for 96 hours followed by analysis of CD38 and
646 HLA-DR expressions.

647 For a proliferation assay, sorted CCR7^{-} memory CD8^{+} T cells were stained with
648 CellTrace Violet (Invitrogen) following the manufacturer's instructions. CellTrace Violet-
649 labelled cells were cultured with IL-15 (10 ng/ml), anti-CD3 (coated, 1 µg/ml), or the
650 combination of both for 96 hours, and then we measured their proliferation and Ki-67
651 expression.
652 We also tested the effects of chemical inhibitors. Sorted CCR7^{-} memory CD8^{+} T cells
653 were pre-treated with everolimus (10 µM; Selleckchem), FK506 (10 ng/ml; Selleckchem), CsA
654 (100 ng/ml; Selleckchem), SP600125 (10 µM; Selleckchem), or SR11302 (10 µM;
655 Selleckchem) for one hour, followed by stimulation with IL-15, anti-CD3, or the combination
656 of both.
657
658 **Flow cytometry**
659 Cells were stained with a mixture of brilliant stain buffer (BD Biosciences) and fluorochrome-
660 conjugated antibodies that bind to surface markers, for 20 min at 4°C. Dead cells were
661 excluded from analysis using the Live/Dead Cell Stain Kit (Invitrogen). To stain intracellular
662 molecules, surface-stained cells were fixed and permeabilized (Invitrogen) for 20 min at 4°C.
663 Subsequently, these cells were stained with fluorochrome-conjugated antibodies targeting
664 intracellular molecules, for 20 min at 4°C. To analyze HCMV- and EBV-specific CD8^{+} T cells,
665 PBMCs were stained with MHC-I dextramers (Immudex) specific for HCMV (HCMV pp65
666 495–504; NLVPMVATV) and EBV (EBV BMLF-1 259–267; GLCTLVAML), and fluorochrome-
667 conjugated monoclonal antibodies for cell surface proteins. Multicolor flow cytometry was
668 performed using LSR II, LSR Fortessa, and FACSymphony A3 instruments (BD Biosciences),
669 and data were analyzed using FlowJo software (Treestar).
670
671 **Quantitative PCR**
672 Total RNA was isolated using Ribospin^{TM} total RNA purification kit (GeneAll). Complementary
673 DNA (cDNA) was synthesized using cDNA synthesis master mix (LeGene). TaqMan Gene
674 Expression Assays (Applied Biosystems) were used to quantify *HCST* mRNA expression, which
675 was normalized to the endogenous control *B2M* expression. Quantitative PCR was

676 performed on a CFX96 Real-Time PCR Detection System and analyzed using CFX Manager™
677 IVD Software (Bio-Rad).
678
679 **Bulk RNA sequencing**
680 Bulk RNA-seq was performed on sorted CCR7⁻ memory CD8⁺ T cells that were stimulated
681 with IL-15, anti-CD3, or the combination of both for 48 hours; or with IL-15, ionomycin, or
682 the combination of both for 12 hours. Total RNA was extracted using TRIZOL reagent
683 (Invitrogen). RNA quality and quantity were evaluated using an Agilent 2100 Bioanalyzer
684 with an RNA 6000 Nano Chip (Agilent Technologies) and an ND-2000 spectrophotometer
685 (Thermo Fisher Scientific), respectively. An RNA library was prepared using a QuantSeq 3'
686 mRNA-seq Library Prep Kit (Lexogen). An individual set of 500 ng total RNA was prepared, an
687 oligo-dT primer containing an Illumina-compatible sequence at its 5' end was hybridized to
688 the RNA, and reverse transcription was performed. After degradation of the RNA template,
689 second strand synthesis was processed using a random primer with an Illumina-compatible
690 linker sequence at its 5' end. Magnetic beads were used to purify the double-stranded
691 library, and to eliminate reactive components. The library was amplified for the addition of
692 complete adapter sequences needed for cluster generation and, finally, the amplified library
693 was purified from PCR components.
694 High-throughput sequencing was performed by single-end 75 sequencing using
695 NextSeq 500 (Illumina). Alignment of the QuantSeq 3' mRNA-Seq reads based on a human
696 reference sequence (hg19) was performed using Bowtie2.[50] Gene counts were normalized
697 according to the library size, and DEGs were analyzed using DESeq2 (v.1.24.0).[51] An
698 experimental batch was corrected using the removeBatchEffect function from limma.[52] DEGs
699 were identified based on two cut-off values: an adjusted *P* value < 0.05, and an absolute log2
700 fold change > 1. GSEA was performed using Broad Institute Software (http://www.gsea-
701 msigdb.org/gsea/index.jsp). For upregulated DEGs, pathway analysis was performed using
702 the enrichR database (https://maayanlab.cloud/Enrichr/). The following pathway databases
703 were utilized in this study: MSigDB Hallmark 2020 (interferon gamma response, interferon
704 alpha response, and TNF-alpha signaling via NF-kB), Reactome 2022 (interferon signaling R-
705 HAS-913531, cell cycle R-HAS-1640170, rRNA processing, cytokine signaling in immune

706 system R-HAS-1280215, innate immune system R-HAS-168249, and interferon alpha/beta
707 signaling R-HAS-909733), KEGG 2021 Human (natural killer cell-mediated cytotoxicity, T-cell
708 receptor signaling pathway, and chemokine signaling pathway), Elsevier Pathway Collection
709 (natural killer cell precursor -> NK cell surface expression markers, natural killer cell
710 activation), NCI-Nature 2016 (calcineurin-regulated NFAT-dependent transcription in
711 lymphocyte), and BioPlanet 2019 (regulation of NFAT transcription factors, MYC active
712 pathway, EGFR1 pathway, T-cell receptor calcium pathway).
713
714 **Cytotoxicity assay**
715 Sorted $CD8^+$ T cells from patients with acute HAV infection were stimulated with IL-15 (10
716 ng/ml) alone or in combination with ionomycin (500 ng/ml) for 24 hours. K562 target cells
717 were labelled with PKH26 (Sigma-Aldrich) following the manufacturer's instructions, and co-
718 cultured with stimulated $CD8^+$ T cells at an effector:target cell ratio of 20:1, for 12 hours. To-
719 Pro-3-iodide (0.5 µM; Invitrogen) was added to the samples, and cells were immediately
720 analyzed by flow cytometry. To obtain the background or maximum To-Pro-3-Iodide staining,
721 target cells were incubated in medium without effector cells or detergent, respectively. The
722 specific cytotoxicity was calculated by extracting the percentage of To-Pro-3-Iodide+ PKH26+
723 cells cultured without effector cells, from the percentage of To-Pro-3-Iodide+ $PKH26^+$ cells in
724 co-culture.
725
726 **siRNA transfection**
727 PBMCs were transfected with c-Jun- or c-Fos-specific small interfering RNA (siRNA)
728 (Invitrogen) or negative control siRNA (Invitrogen) using the Neon NxT electroporation
729 system (Invitrogen). Transfection was performed with 200 nM siRNA at 2000 V for three 10
730 ms pulses. Following transfection, PBMCs were cultured in RPMI 1640 medium (Corning)
731 supplemented with 10% fetal bovine serum (Corning) without antibiotics for 4 days.
732 Subsequently, PBMCs were treated with IL-15 (10 ng/ml) for 48 hours, and expression of
733 NKG2D was analyzed on $CCR7^-$ memory $CD8^+$ T cells by flow cytometry.
734
735 **NFATc1 plasmids transfection**

736 pcDNA3.1 plasmid containing wild-type and T551A mutant[24] NFATc1 were purchased from
737 Genescript. PBMCs were transfected with empty pcDNA3.1 plasmids or plasmids containing
738 wild-type and T551A mutant NFATc1 using the Neon NxT electroporation system.
739 Transfection was performed with 5 µg of plasmids at 2000 V for a single 20 ms pulse.
740 Subsequently, PBMCs were cultured with IL-15 (10 ng/ml) for 48 hours and expression of
741 NKG2D was analyzed on CCR7$^-$ memory CD8$^+$ T cells by flow cytometry.
742
743 **ChIP-qPCR**
744 Sorted CCR7$^-$ memory CD8$^+$ T cells were stimulated with IL-15 (10 ng/ml) or IL-15 with anti-
745 CD3 (coated, 1 µg/ml) for 48 hours. Cells were double cross-linked with 2mM DSG (Thermo
746 Fisher) and 1% formaldehyde (Sigma-Aldrich) at room temperature for 35 min and 10 min,
747 respectively. Cells were then lysed with 1% SDS buffer (1% SDS, 10 mM EDTA, 50 mM Tris pH
748 8.1) and chromatin was fractionated by sonication (Covaris, S220). The lysate was diluted
749 with dilution buffer and incubated with pre-coated Dynabeads Protein A (Thermo Fisher)
750 with c-Jun antibody (Abcam) and IgG (Abcam) as negative control overnight at 4°C with
751 rotation. A portion of diluted lysate was stored to quantify the total amount of DNA in each
752 sample as input control. The immunoprecipitated chromatin was washed four times with
753 RIPA buffer (140 mM NaCl, 1 mM EDTA, 0.5 Mm EGTA, 1% Triton X-100, 0.1% SDS, 0.1%
754 sodium deoxycholate, 10 mM Tris pH 8.0) and incubated with RNase A (Thermo Fisher) and
755 proteinase K (New England Biolabs) overnight at 65°C to reverse crosslink. The
756 immunoprecipitated DNA was purified by AMPure XP beads (Beckman, A63881) and
757 analyzed by Real-Time PCR using primers designed based on open chromatin regions
758 identified from publicly available ATAC-seq data[53] and AP-1 ChIP data[54] (*HCST*: FW –
759 CAGCAAATTTTCTTGGCCCTACCTC, RV – GTTACTGCCTTTGGTGAACGA; *IFITM3*: FW –
760 GGGGGAATCTCAAAAGGCCA, RV – TGGGCCCATGTTCTCAAGAC; *CCR5*: FW –
761 TTGGGTGGTGAGCATCTGTG, RV – TGTAGAGGGGGATCCTGGAC).
762
763 **scRNA-seq library preparation and sequencing**
764 Sorted CD8$^+$ T cells from PBMCs of patients (n = 5) at acute and convalescent stages of HAV
765 infection and healthy donors (n = 3) were stained with PE-conjugated MHC-I dCODE

766 dextramers (Immudex) specific for HLA-A*0201 HAV $3D_{2026}$ LLYNCCYHV, HLA-A*0201 HCMV
767 $pp65_{495}$ NLVPMVATV, HLA-A*0201 EBV $BMLF1_{259}$ GLCTLVAML, and HLA-A*0201 IAV MP_{58}
768 GILGFVFTL. Subsequently, these cells were sorted into dCODE-positive and -negative $CD8^+$ T
769 cells using a FACSAria II instrument (BD Biosciences). The sorted cells were mixed at a 1:9
770 ratio, and then further stained with CITE-seq antibodies (TotalSeq-C; Biolegend). Cell
771 suspensions were pelleted, and scRNA-seq libraries were prepared using the Chromium
772 Single Cell 5' Library & Gel Bead Kit (PN-10000006) and 5' Feature Barcode Library Kit (PN-
773 1000020) (10X Genomics), following the manufacturer's instructions. These libraries were
774 sequenced at a depth of approximately 20,000 reads per cell for genes and ADTs using the
775 NovaSeq6000 platform (Illumina).
776
777 **Single-cell transcriptome and ADT expression analysis**
778 Fastq files were generated by demultiplexing the sequenced data using the mkfastq function
779 (Cell Ranger, 10X Genomics, v3.1.0). The demultiplexed fastq files for the expressions of each
780 gene and ADT were aligned to the reference human genome (GRCH38; 10X Cell Ranger
781 reference GRCh38 v3.0.0). The barcode sequencing of each ADT and dCODE dextramer,
782 filtering, barcode counting, and UMI counting were performed to generate feature-barcode
783 matrices using the count function (Cell Ranger, v3.1.0). For basic quality control, we filtered
784 out low-quality cells with mitochondrial genes constituting >10% of their total gene
785 expression, <300 genes or >5,500 genes, or UMI counts of <500 or >55,000. Next, we
786 identified highly variable genes by standardizing the normalization of gene expression in
787 each cell based on the total read count. To correct for a batch effect and harmonize the
788 datasets, we identified 'anchor' vectors of genes using the FindIntegrationAnchors function,
789 and integrated the datasets using the IntegrateData function (Seurat, v3.2.2).[55] The
790 integrated samples were scaled using the ScaleData function (Seurat), and PCA was
791 conducted using the RunPCA function (Seurat) for dimensional reduction. Lastly, the cells
792 were visualized by UMAP using the top 20 principal components (PCs) with the RunUMAP
793 function (Seurat) for whole-cell types. Enrichment of bulk RNA-seq data on scRNA-seq data
794 was performed by measuring the enrichment score with the Addmodulescore function

795 (Seurat). The pseudo-bulk scRNA-seq data were obtained using the AggregateExpression
796 function (Seurat).
797
798 **Analysis of a public RNA-seq dataset**
799 We re-analyzed publicly available bulk RNA-seq datasets for bystander-activated $CD8^+$ T cells
800 from a mouse model of influenza infection[20] (SRX13530605, SRX13530604, SRX13530603,
801 SRX13530601, and SRX13530600ref). Orthologous pairs of human and mouse genes were
802 processed using the getLDS function (biomaRt).[56] Enrichment of upregulated DEGs from the
803 current study in the public data was performed using the fgsea package
804
805 **Statistical analysis**
806 Statistical analyses were performed using GraphPad Prism (GraphPad Software version 8.4)
807 or R software (R Foundation for Statistical Computing). The paired t test was used to
808 compare continuous variables. The Mann–Whitney U test was used to compare data
809 between two unpaired groups, and the Wilcoxon signed-rank test was used to compare data
810 between two paired groups, and one-way ANOVA with Tukey's correction was used to
811 compare multiple groups. Two-sided *P* values were determined in all analyses, and a *P* value
812 < 0.05 was considered significant.

Figure 1

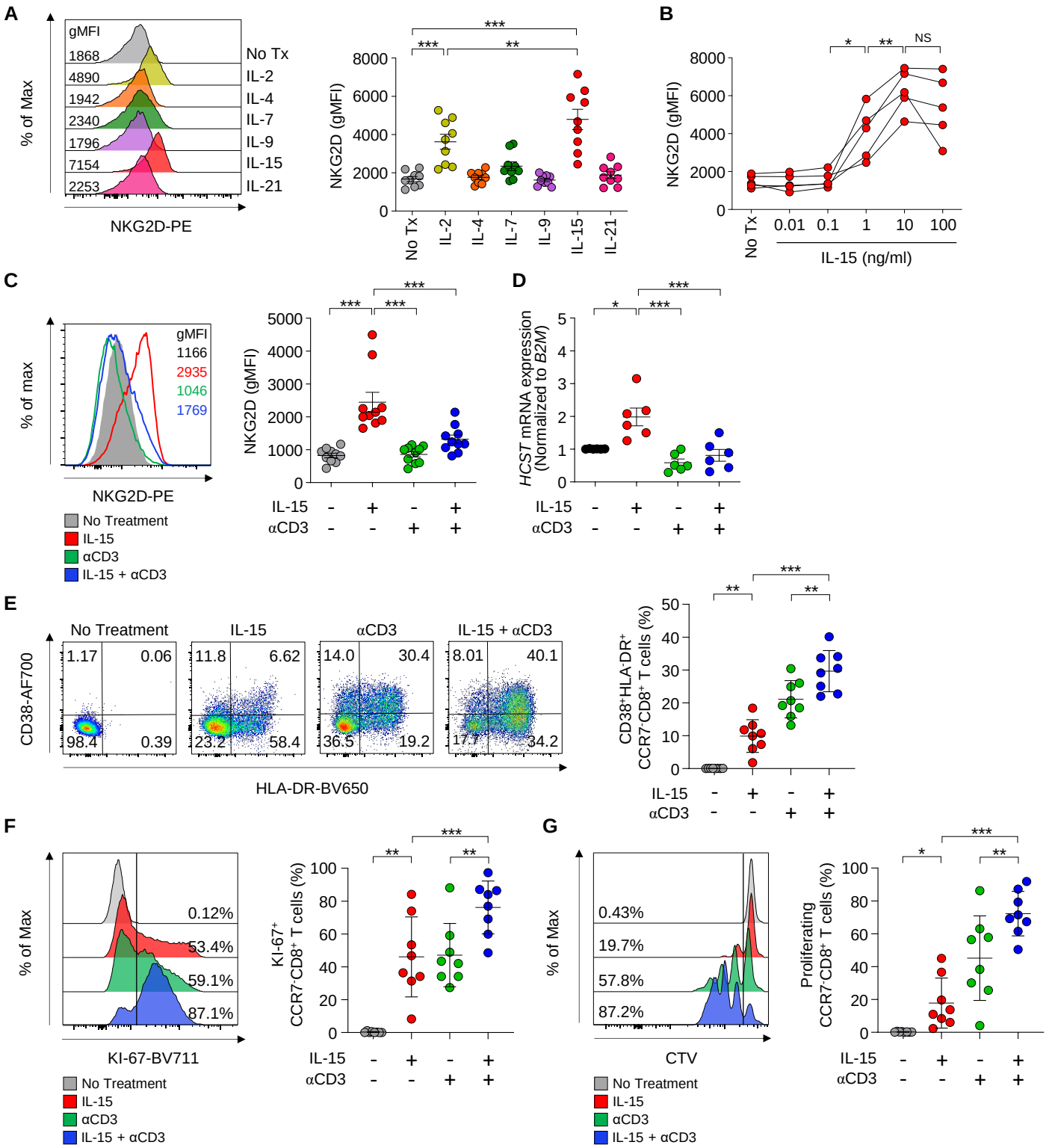

Figure 1. IL-15-induced upregulation of NKG2D on memory CD8⁺ T cells, which is counteracted by concurrent TCR stimulation. (A and B) Peripheral blood mononuclear cells (PBMCs) from healthy donors (n = 9) were stimulated for 48 hours with IL-2 (10 ng/ml), IL-4 (10 ng/ml), IL-7 (10 ng/ml), IL-9 (10 ng/ml), IL-15 (10 ng/ml) or IL-21 (50 ng/ml). (A) Representative flow cytometry stacked histograms and cumulative data presenting NKG2D expression on CCR7⁻ memory CD8⁺ T cells from healthy donor PBMCs following stimulation with the indicated cytokines. (B) Cumulative data presenting NKG2D expression on CCR7⁻ memory CD8⁺ T cells stimulated for 48 hours with varying doses of IL-15 (0.01, 0.1, 1, 10, and 100 ng/ml). **(C and D)** Sorted CCR7⁻ memory CD8⁺ T cells from healthy donors were stimulated with IL-15 (10 ng/ml), anti-CD3 (coated, 1 µg/ml), or the combination of both for 48 hours. (C) Representative stacked flow cytometry histograms and cumulative data presenting the expression of NKG2D (n = 10). (D) mRNA levels of *HCST* (n = 6) measured by qPCR with specific primer sets and normalized to *B2M* expression. **(E)** Representative flow cytometry plots and cumulative data presenting the expression CD38 and HLA-DR (n = 8) on CCR7⁻ memory CD8⁺ T cells stimulated in the same way as in (C), but for 96 hours. **(F and G)** Sorted CCR7⁻ memory CD8⁺ T cells from healthy donors (n = 8) were stained with CellTrace Violet, and stimulated with IL-15 (10 ng/ml), anti-CD3 (coated, 1 µg/ml), or the combination of both for 96 hours. Representative stacked flow cytometry histograms and cumulative data present (F) Ki-67 expression and (G) proliferation of CCR7⁻ memory CD8⁺ T cells. Error bars represent mean ± SD. Statistical analysis was performed using the paired Student's t test. NS, not significant, *P < 0.05, **P < 0.01, ***P < 0.001.

Figure 2

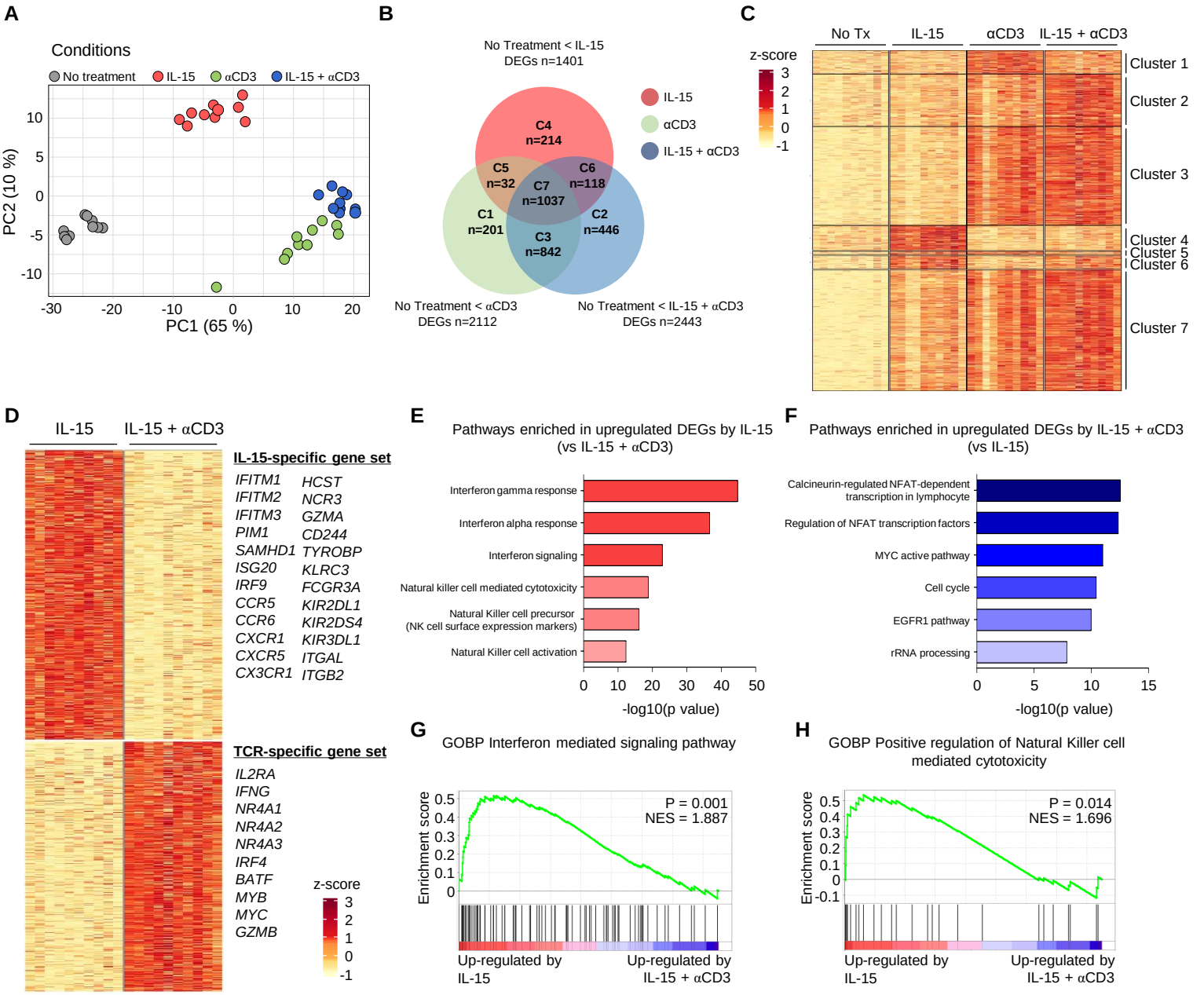

Figure 2. Transcriptional profiles of memory CD8⁺ T cells stimulated with IL-15, anti-CD3, or the combination of both. (A-H) Sorted CCR7⁻ memory CD8⁺ T cells from healthy donors (n = 10) were stimulated for 48 hours with IL-15 (10 ng/ml), anti-CD3 (coated, 1 µg/ml), or the combination of both. Total RNA was isolated and RNA-seq was performed. **(A)** Principal component analysis (PCA) indicating segregation of the gene expression patterns of memory CD8⁺ T cells stimulated with IL-15, anti-CD3, or the combination of both. **(B)** Venn diagram of individual and overlapping differentially expressed genes of memory CD8⁺ T cells stimulated with IL-15, anti-CD3, or the combination of both, compared to unstimulated cells and **(C)** Heat-map showing the z scores of normalized read counts (adjusted $P < 0.05$, Log2 fold-change > 1). **(D)** Heat-map of differentially expressed genes between memory CD8⁺ T cells stimulated with IL-15 alone or IL-15 plus anti-CD3 (adjusted $P < 0.05$, Log2 fold-change > 1). **(E and F)** Bar-plots showing the enrichment scores (−log10[p value]) of various pathways enriched in DEGs upregulated by (E) IL-15 or (F) IL-15 plus anti-CD3. **(G and H)** GSEA of (G) GOBP interferon-mediated signaling pathway (GO: 0140888) and (H) GOBP positive regulation of natural killer-cell-mediated cytotoxicity (GO: 0045954) in memory CD8⁺ T cells stimulated with IL-15 alone versus IL-15 plus anti-CD3.

Figure 3

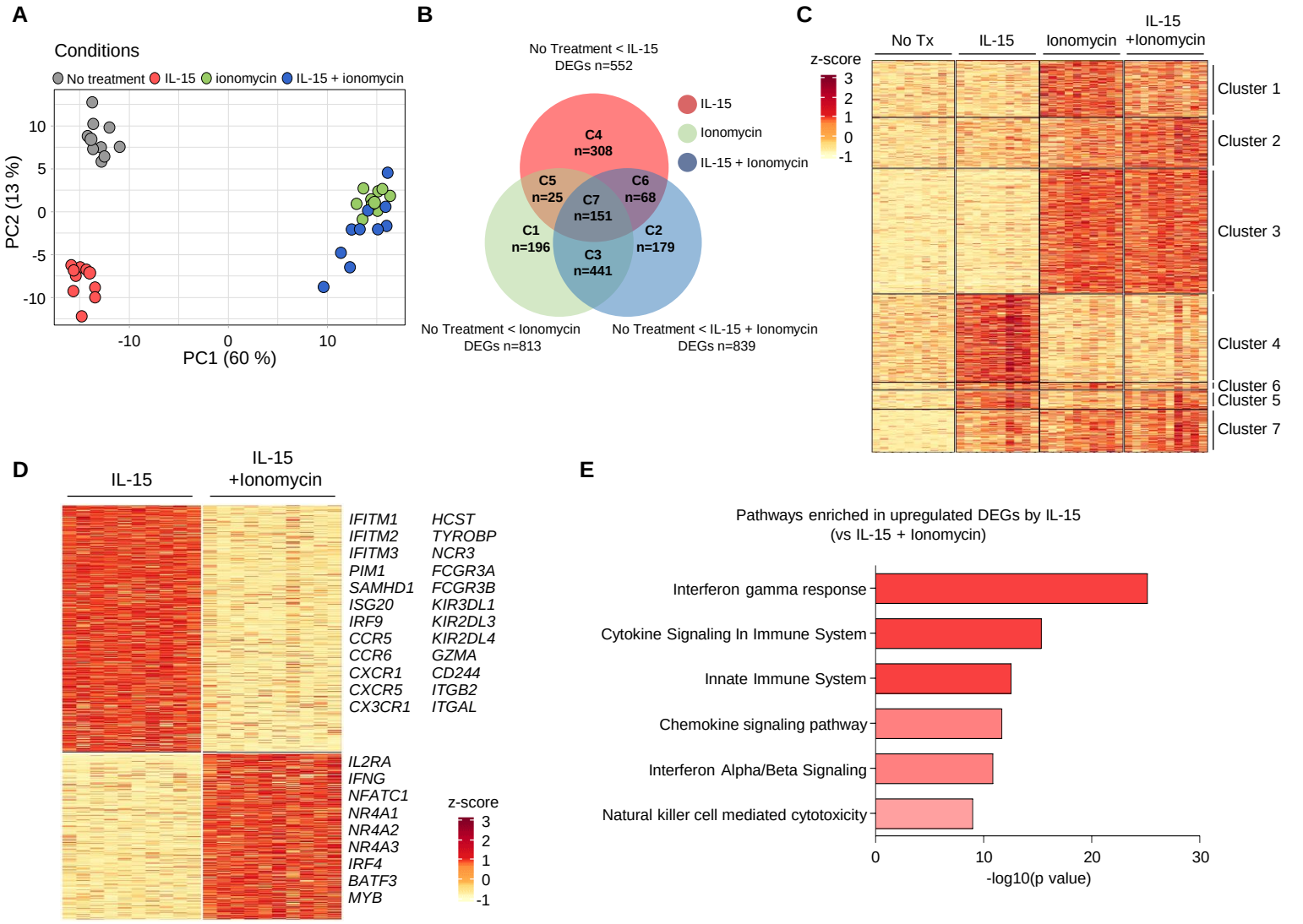

Figure 3. Transcriptional profiles of memory CD8⁺ T cells stimulated with IL-15, ionomycin, or the combination of both. (A-E) Sorted CCR7⁻ memory CD8⁺ T cells from healthy donors (n = 10) were stimulated for 12 hours with IL-15 (10 ng/ml), ionomycin (500 ng/ml), or the combination of both. Total RNA was isolated and RNA-seq was performed. **(A)** PCA indicating segregation of gene expression patterns of memory CD8⁺ T cells stimulated with IL-15, ionomycin, or the combination of both. **(B)** Venn diagram of individual and overlapping differentially expressed genes of memory CD8⁺ T cells stimulated with IL-15, ionomycin, or the combination of both compared to unstimulated cells and **(C)** Heat-map showing the z scores of normalized read counts (adjusted $P < 0.05$, Log2 fold-change > 1). **(D)** Heat-map of differentially expressed genes between memory CD8⁺ T cells stimulated with IL-15 or with IL-15 plus ionomycin (adjusted $P < 0.05$, Log2 fold-change > 1). **(E)** Bar-plots showing the enrichment scores (−log10[p value]) of various pathways enriched in DEGs upregulated by IL-15 and down-regulated by IL-15 plus ionomycin. Statistical analysis was performed using the paired Student's t test. ****$P < 0.0001$.

Figure 4

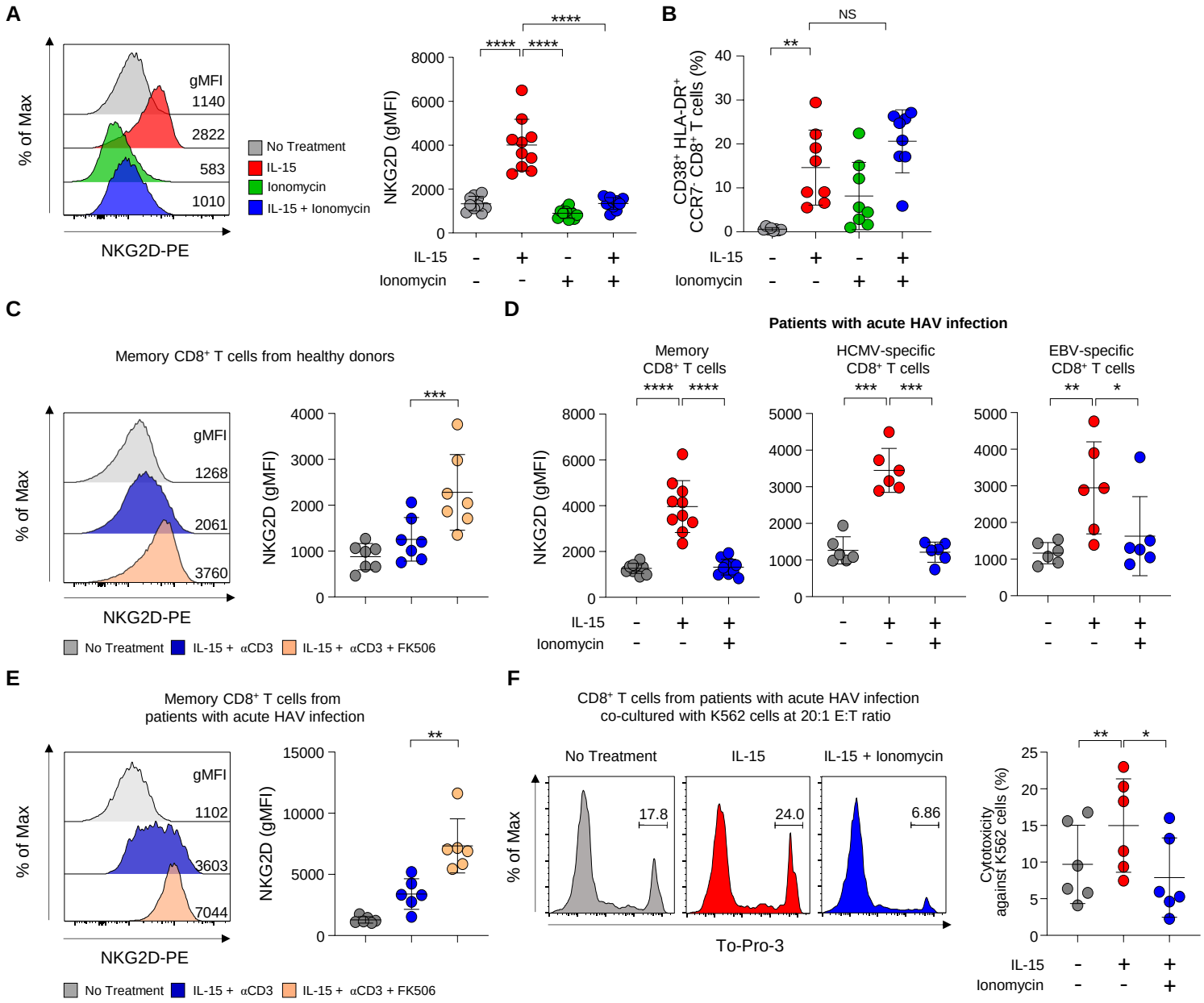

Figure 4. The role of Ca^{2+}-calcineurin signaling on IL-15-induced NK-like cytotoxicity of $CD8^+$ T cells. (A and B) Sorted $CCR7^-$ memory $CD8^+$ T cells from healthy donors were stimulated with IL-15 (10 ng/ml), ionomycin (500 ng/ml), or the combination of both. (A) Representative stacked flow cytometry histograms and cumulative data presenting the expression of NKG2D (n = 10) on $CCR7^-$ memory $CD8^+$ T cells after 48 hours of stimulation. (B) Cumulative data presenting expression of CD38 and HLA-DR (n = 8) on $CCR7^-$ memory $CD8^+$ T cells after 96 hours of stimulation. **(C)** Sorted $CCR7^-$ memory $CD8^+$ T cells from healthy donors (n = 7) were pretreated with FK506 (10 ng/ml) for 1 hour, followed by stimulation with IL-15 (10 ng/ml) and anti-CD3 (coated, 1 µg/ml) for 48 hours. Representative stacked flow cytometry histograms and cumulative data present NKG2D expression on $CCR7^-$ memory $CD8^+$ T cells. **(D)** PBMCs from patients with acute HAV infection were stimulated with IL-15 (10 ng/ml) or a combination of IL-15 plus ionomycin (500 ng/ml) for 48 hours. Cumulative data present NKG2D expression on $CCR7^-$ memory (n = 10), HCMV-specific (n = 6), and EBV-specific (n = 6) $CD8^+$ T cells. **(E)** Sorted $CCR7^-$ memory $CD8^+$ T cells from patients with acute HAV infection (n = 6) were pretreated with FK506 (10 ng/ml) for 1 hour, followed by stimulation with IL-15 (10 ng/ml) and anti-CD3 (coated, 1 µg/ml) for 48 hours. Representative stacked flow cytometry histograms and cumulative data present NKG2D expression on $CCR7^-$ memory $CD8^+$ T cells. **(F)** Sorted total $CD8^+$ T cells from patients with acute HAV infection (n = 6) were stimulated with IL-15 (10 ng/ml) or a combination of IL-15 plus ionomycin (500 ng/ml) for 24 hours, and co-cultured with PKH-26-labeled K562 cells at a 20:1 effector:target cell (E:T) ratio for 12 hours. Cytotoxicity was analyzed by flow cytometry following staining of the dead cells with TO-PRO-3 and presented as representative histograms and cumulative data. Error bars represent mean ± SD. Statistical analysis was performed using the paired Student's t test. *$P < 0.05$, **$P < 0.01$, ***$P < 0.001$, ****$P < 0.0001$.

Figure 5

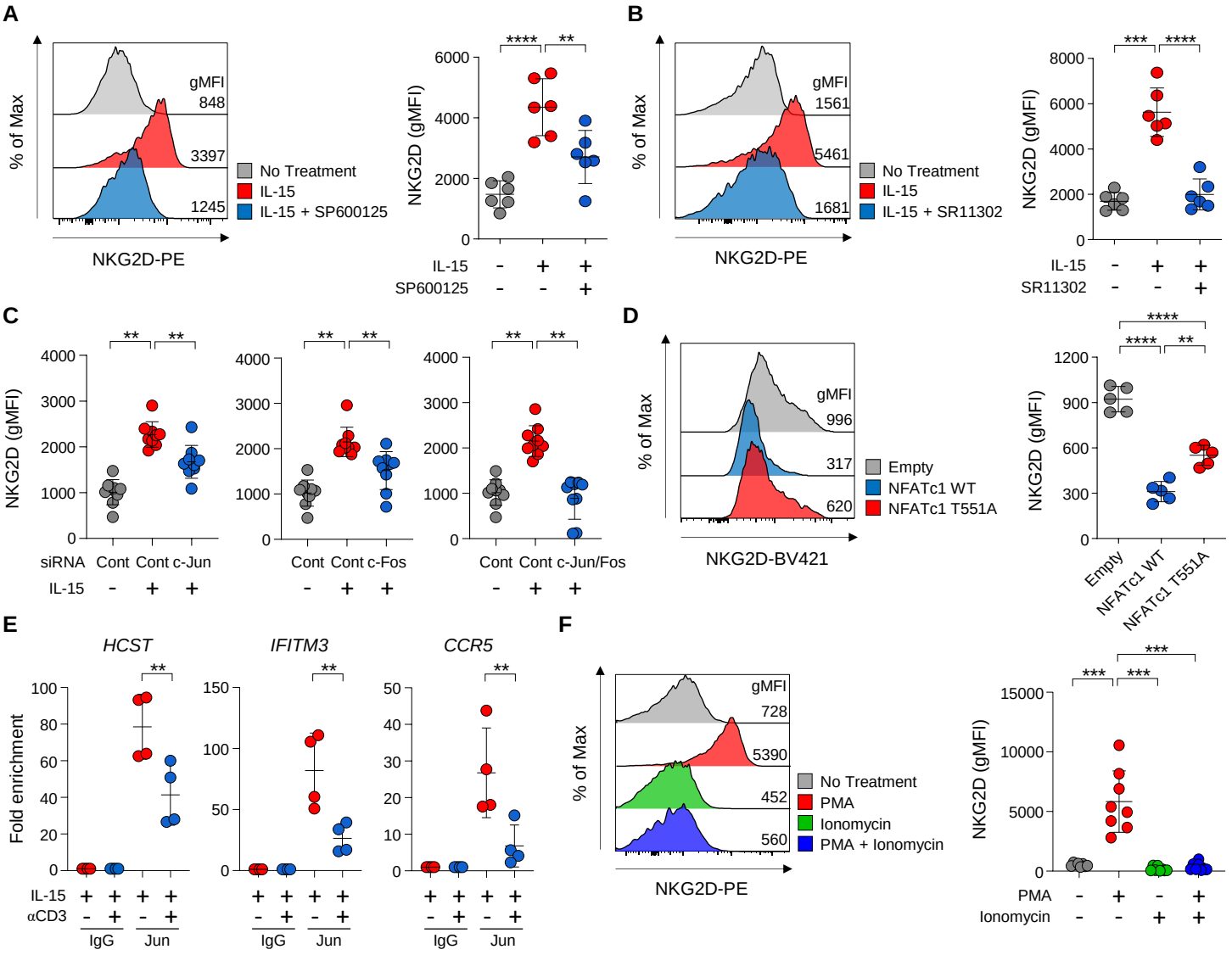

Figure 5. NFATc1-mediated suppression of IL-15-induced NKG2D upregulation through AP-1 binding. (A and B) PBMCs from healthy donors (n = 6) were pretreated with SP600125 (10 µM) or SR11302 (10 µM) for 1 hour, followed by stimulation with IL-15 (10 ng/ml) for 48 hours. Representative stacked flow cytometry histograms and cumulative data present NKG2D expression on CCR7⁻ memory CD8⁺ T cells pretreated with (A) SP600125 or (B) SR11302. **(C)** PBMCs from healthy donors (n = 9) were transfected with c-Jun siRNA (200 nM), c-fos siRNA (200 nM) or the combination of both siRNAs and rested for 4 days. Subsequently, PBMCs were stimulated with IL-15 (10 ng/ml) for 48 hours. Cumulative data present NKG2D expression on CCR7⁻ memory CD8⁺ T cells. **(D)** PBMCs from healthy donors (n = 5) were transfected with pcDNA3.1 plasmids containing wild-type or T551A mutant NFATc1. Subsequently, PBMCs were stimulated with IL-15 (10 ng/ml) for 48 hours. Representative stacked flow cytometry histograms and cumulative data present NKG2D expression on CCR7⁻ memory CD8⁺ T cells. **(E)** ChIP-qPCR assays for Jun occupancy at the highly open chromatin genetic regions of *HCST*, *IFITM3* or *CCR5* in sorted CCR7⁻ memory CD8⁺ T cells from healthy donors (n = 4) stimulated for 48 hours with IL-15 (10 ng/ml), anti-CD3 (coated, 1 µg/ml), or the combination of both. The y-axis represents fold enrichment, calculated as the fold change of immunoprecipitated DNA with c-Jun relative to immunoprecipitated DNA with IgG, analyzed by ChIP-qPCR using the primers described in the methods section. **(F)** Sorted CCR7⁻ memory CD8⁺ T cells from healthy donors (n = 8) were stimulated with PMA (10 ng/ml), ionomycin (500 ng/ml), or the combination of both for 48 hours. Representative stacked flow cytometry histograms and cumulative data present NKG2D expression on CCR7⁻ memory CD8⁺ T cells. Error bars represent mean ± SD. Statistical analysis was performed using the paired Student's t test for (A) to (D) and (F) and one-way ANOVA test for (E). **P < 0.01, ***P < 0.001, ****P < 0.0001.

Figure 6

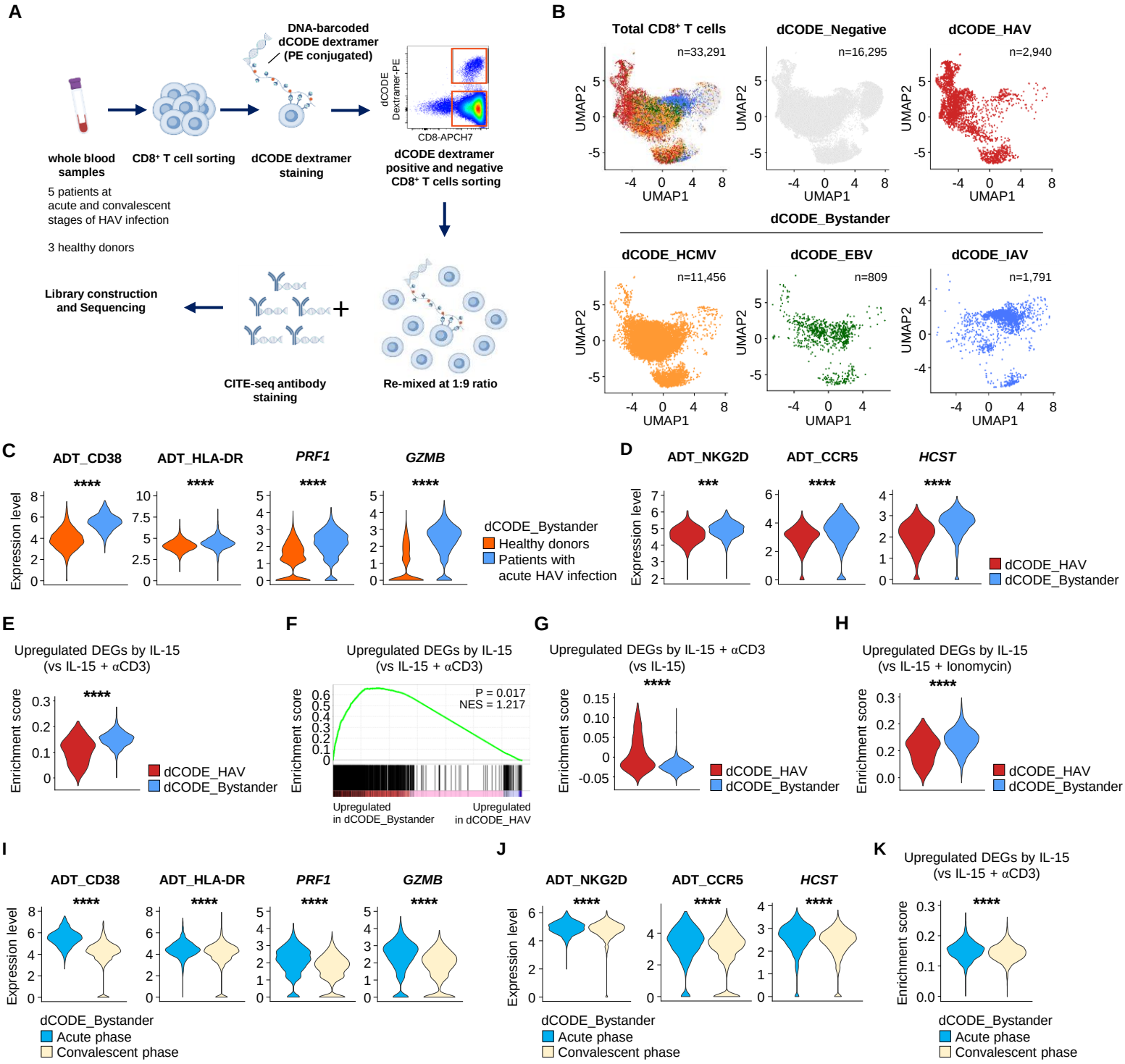
A
DNA-barcoded dCODE dextramer (PE conjugated)
dCODE Dextramer-PE
CD8-APCH7
whole blood samples
CD8+ T cell sorting
dCODE dextramer staining
dCODE dextramer positive and negative CD8+ T cells sorting
5 patients at acute and convalescent stages of HAV infection
3 healthy donors
Library construction and Sequencing
CITE-seq antibody staining
Re-mixed at 1:9 ratio
B
Total CD8+ T cells
n=33,291
dCODE_Negative
n=16,295
dCODE_HAV
n=2,940
dCODE_Bystander
dCODE_HCMV
n=11,456
dCODE_EBV
n=809
dCODE_IAV
n=1,791
UMAP1
UMAP2
C
ADT_CD38
ADT_HLA-DR
PRF1
GZMB
Expression level
dCODE_Bystander
Healthy donors
Patients with acute HAV infection
D
ADT_NKG2D
ADT_CCR5
HCST
dCODE_HAV
dCODE_Bystander
E
Upregulated DEGs by IL-15 (vs IL-15 + αCD3)
Enrichment score
F
P = 0.017
NES = 1.217
Upregulated in dCODE_Bystander
Upregulated in dCODE_HAV
G
Upregulated DEGs by IL-15 + αCD3 (vs IL-15)
H
Upregulated DEGs by IL-15 (vs IL-15 + Ionomycin)
I
J
K
Acute phase
Convalescent phase

Figure 6 (continued)

Figure 6. High-throughput single-cell analysis of virus-specific CD8$^+$ T cells from patients with HAV infection. (A-K) Total CD8$^+$ T cells were isolated from patients at acute and convalescent stages of HAV infection (n = 5) and healthy donors (n = 3) by magnetic separation, and stained with DNA barcode-labeled MHC class I dextramers conjugated with PE (dCODE dextramers). dCODE dextramer-positive and -negative CD8$^+$ T cells were flow-sorted, and then re-mixed at a 1:9 ratio and further stained with ADTs. Subsequently, these cells were processed for single-cell RNA sequencing. **(A)** Schematic overview of the experimental design. **(B)** UMAP projections of 33,291 total CD8$^+$ T cells, including dCODE-negative (n = 16,295) and HAV-specific CD8$^+$ T cells (n = 2,940), and bystander CD8$^+$ T cells, including HCMV-specific (n = 11,456), EBV-specific (n = 809) and IAV-specific (n = 1,791) CD8$^+$ T cells. **(C)** Violin plots showing ADT expression of CD38 and HLA-DR, and normalized gene expression of *PRF1* and *GZMB* in bystander (CMV-, EBV- and IAV-specific) CD8$^+$ T cells from patients with acute HAV infection versus those from healthy donors. **(D)** ADT expression of NKG2D and CCR5, and normalized gene expression of *HCST* in HAV-specific versus bystander CD8$^+$ T cells from patients with acute HAV infection. **(E)** Violin plot showing enrichment score for DEGs upregulated by IL-15 compared to IL-15 plus anti-CD3 in memory CD8$^+$ T cells, analyzed in HAV-specific and bystander CD8$^+$ T cells from patients with acute HAV infection. **(F)** GSEA of upregulated DEGs from IL-15-stimulated memory CD8$^+$ T cells, using the transcriptomes of HAV-specific versus bystander CD8$^+$ T cells from patients with acute HAV infection obtained using a pseudo bulk approach. **(G)** Violin plot showing enrichment score for DEGs upregulated by IL-15 plus anti-CD3 compared to IL-15 alone in memory CD8$^+$ T cells, analyzed in HAV-specific and bystander CD8$^+$ T cells from patients with acute HAV infection. **(H)** Violin plot showing enrichment score for DEGs upregulated by IL-15 compared to IL-15 plus ionomycin in memory CD8$^+$ T cells, analyzed in HAV-specific and bystander CD8$^+$ T cells from patients with acute HAV infection. **(I and J)** Violin plots showing (I) ADT expression of CD38 and HLA-DR, and normalized gene expression of *PRF1* and *GZMB*, and (J) ADT expression of NKG2D and CCR5, and normalized gene expression of *HCST* in bystander CD8$^+$ T cells from patients at the acute and convalescent stages of HAV infection. **(K)** Violin plot showing enrichment score for DEGs upregulated by IL-15 compared to IL-15 plus anti-CD3 in memory CD8$^+$ T cells, analyzed in bystander CD8$^+$ T cells from patients at the acute and convalescent stages of HAV infection. Statistical analysis was performed using the Mann-Whitney U-test ***$P < 0.001$, ****$P < 0.0001$.

813 **References**

814 1. Kaech, S.M., Wherry, E.J. & Ahmed, R. Effector and memory T-cell differentiation:
815 implications for vaccine development. *Nat Rev Immunol*. **2**, 251-262 (2002).
816 2. Lee, H., Jeong, S. & Shin, E.C. Significance of bystander T cell activation in microbial
817 infection. *Nat Immunol*. **23**, 13-22 (2022).
818 3. Maurice, N.J., Taber, A.K. & Prlic, M. The Ugly Duckling Turned to Swan: A Change in
819 Perception of Bystander-Activated Memory CD8 T Cells. *J Immunol*. **206**, 455-462 (2021).
820 4. Zhang, X.H., Sun, S.Q., Hwang, I.K., Tough, D.F. & Sprent, J. Potent and selective
821 stimulation of memory-phenotype CD8(+) T cells in vivo by IL-15. *Immunity*. **8**, 591-599
822 (1998).
823 5. Meresse, B. et al. Coordinated induction by IL15 of a TCR-independent NKG2D signaling
824 pathway converts CTL into lymphokine-activated killer cells in celiac disease. *Immunity*.
825 **21**, 357-366 (2004).
826 6. Soudja, S.M., Ruiz, A.L., Marie, J.C. & Lauvau, G. Inflammatory monocytes activate
827 memory CD8(+) T and innate NK lymphocytes independent of cognate antigen during
828 microbial pathogen invasion. *Immunity*. **37**, 549-562 (2012).
829 7. Younes, S.A. et al. IL-15 promotes activation and expansion of CD8+ T cells in HIV-1
830 infection. *J Clin Invest*. **126**, 2745-2756 (2016).
831 8. Kim, J. et al. Innate-like Cytotoxic Function of Bystander-Activated CD8(+) T Cells Is
832 Associated with Liver Injury in Acute Hepatitis A. *Immunity*. **48**, 161-173 e165 (2018).
833 9. Sandalova, E. et al. Contribution of herpesvirus specific CD8 T cells to anti-viral T cell
834 response in humans. *PLoS Pathog*. **6**, e1001051 (2010).
835 10. Leem, G. et al. Tumour-infiltrating bystander CD8(+) T cells activated by IL-15 contribute
836 to tumour control in non-small cell lung cancer. *Thorax*. **77**, 769-780 (2022).
837 11. Chu, T. et al. Bystander-activated memory CD8 T cells control early pathogen load in an
838 innate-like, NKG2D-dependent manner. *Cell Rep*. **3**, 701-708 (2013).
839 12. Ge, C. et al. Bystander Activation of Pulmonary Trm Cells Attenuates the Severity of
840 Bacterial Pneumonia by Enhancing Neutrophil Recruitment. *Cell Rep*. **29**, 4236-4244
841 e4233 (2019).

842 13. Sckisel, G.D. et al. Influenza infection results in local expansion of memory CD8(+) T cells
843 with antigen non-specific phenotype and function. *Clin Exp Immunol*. **175**, 79-91 (2014).
844 14. Arkatkar, T. et al. Memory T cells possess an innate-like function in local protection from
845 mucosal infection. *J Clin Invest*. **133** (2023).
846 15. Ostler, T., Pircher, H. & Ehl, S. "Bystander" recruitment of systemic memory T cells delays
847 the immune response to respiratory virus infection. *Eur J Immunol*. **33**, 1839-1848
848 (2003).
849 16. Crosby, E.J., Goldschmidt, M.H., Wherry, E.J. & Scott, P. Engagement of NKG2D on
850 bystander memory CD8 T cells promotes increased immunopathology following
851 Leishmania major infection. *PLoS Pathog*. **10**, e1003970 (2014).
852 17. Crosby, E.J., Clark, M., Novais, F.O., Wherry, E.J. & Scott, P. Lymphocytic Choriomeningitis
853 Virus Expands a Population of NKG2D+CD8+ T Cells That Exacerbates Disease in Mice
854 Coinfected with Leishmania major. *J Immunol*. **195**, 3301-3310 (2015).
855 18. Huang, C.H. et al. Innate-like bystander-activated CD38(+) HLA-DR(+) CD8(+) T cells play
856 a pathogenic role in patients with chronic hepatitis C. *Hepatology*. **76**, 803-818 (2022).
857 19. Seo, I.H. et al. IL-15 enhances CCR5-mediated migration of memory CD8(+) T cells by
858 upregulating CCR5 expression in the absence of TCR stimulation. *Cell Rep*. **36**, 109438
859 (2021).
860 20. Jeong, S. et al. IFITM3 Is Upregulated Characteristically in IL-15-Mediated Bystander-
861 Activated CD8(+) T Cells during Influenza Infection. *J Immunol*. **208**, 1901-1911 (2022).
862 21. Park Y.P. et al. Complex regulation of human NKG2D-DAP10 cell surface expression:
863 opposing roles of the γc cytokines and TGF-β1. *Blood*. **118**, 3019-3027 (2011).
864 22. Lewis, R.S. Calcium signaling mechanisms in T lymphocytes. *Annu Rev Immunol*. **19**, 497-
865 521 (2001).
866 23. Chatila, T., Silverman, L., Miller, R. & Geha, R. Mechanisms of T cell activation by the
867 calcium ionophore ionomycin. *J Immunol*. **143**, 1283-1289 (1989).
868 24. Sun, L.J., Peterson B.R. & Verdine G.L. Dual role of the nuclear factor of activated T cells
869 insert region in DNA recognition and cooperative contacts to activator protein 1.
870 *Proceedings of the National Academy of Sciences*. **94**, 4919-4924 (1997).

871 25. Lodolce, J.P. et al. IL-15 receptor maintains lymphoid homeostasis by supporting
872 lymphocyte homing and proliferation. *Immunity*. **9**, 669-676 (1998).
873 26. Kennedy, M.K. et al. Reversible defects in natural killer and memory CD8 T cell lineages
874 in interleukin 15-deficient mice. *J Exp Med*. **191**, 771-780 (2000).
875 27. Becker, T.C. et al. Interleukin 15 is required for proliferative renewal of virus-specific
876 memory CD8 T cells. *J Exp Med*. **195**, 1541-1548 (2002).
877 28. Goldrath, A.W. et al. Cytokine requirements for acute and Basal homeostatic
878 proliferation of naive and memory CD8+ T cells. *J Exp Med*. **195**, 1515-1522 (2002).
879 29. Geginat, J., Lanzavecchia, A. & Sallusto, F. Proliferation and differentiation potential of
880 human CD8+ memory T-cell subsets in response to antigen or homeostatic cytokines.
881 *Blood*. **101**, 4260-4266 (2003).
882 30. Correia, M.P. et al. Hepatocytes and IL-15: a favorable microenvironment for T cell
883 survival and CD8+ T cell differentiation. *J Immunol*. **182**, 6149-6159 (2009).
884 31. Correia, M.P., Costa, A.V., Uhrberg, M., Cardoso, E.M. & Arosa, F.A. IL-15 induces CD8+ T
885 cells to acquire functional NK receptors capable of modulating cytotoxicity and cytokine
886 secretion. *Immunobiology*. **216**, 604-612 (2011).
887 32. Liu, K., Catalfamo, M., Li, Y., Henkart, P.A. & Weng, N.P. IL-15 mimics T cell receptor
888 crosslinking in the induction of cellular proliferation, gene expression, and cytotoxicity in
889 CD8+ memory T cells. *Proc Natl Acad Sci U S A*. **99**, 6192-6197 (2002).
890 33. Balin, S.J. et al. Human antimicrobial cytotoxic T lymphocytes, defined by NK receptors
891 and antimicrobial proteins, kill intracellular bacteria. *Sci Immunol*. **3** (2018).
892 34. Seok, J. et al. A virtual memory CD8(+) T cell-originated subset causes alopecia areata
893 through innate-like cytotoxicity. *Nat Immunol*. **24**, 1308-1317 (2023).
894 35. Jabri, B. & Abadie, V. IL-15 functions as a danger signal to regulate tissue-resident T cells
895 and tissue destruction. *Nat Rev Immunol*. **15**, 771-783 (2015).
896 36. Ma, S., Caligiuri, M.A. & Yu, J. Harnessing IL-15 signaling to potentiate NK cell-mediated
897 cancer immunotherapy. *Trends Immunol*. **43**, 833-847 (2022).
898 37. Mishra, A., Sullivan, L. & Caligiuri, M.A. Molecular pathways: interleukin-15 signaling in
899 health and in cancer. *Clin Cancer Res*. **20**, 2044-2050 (2014).

900 38. Smith-Garvin, J.E., Koretzky, G.A. & Jordan, M.S. T cell activation. *Annu Rev Immunol*. **27**,
901 591-619 (2009).
902 39. Roberts, A.I. et al. NKG2D receptors induced by IL-15 costimulate CD28-negative effector
903 CTL in the tissue microenvironment. *J Immunol*. **167**, 5527-5530 (2001).
904 40. Deshpande, P. et al. IL-7- and IL-15-mediated TCR sensitization enables T cell responses
905 to self-antigens. *J Immunol*. **190**, 1416-1423 (2013).
906 41. Richer, M.J. et al. Inflammatory IL-15 is required for optimal memory T cell responses. *J*
907 *Clin Invest*. **125**, 3477-3490 (2015).
908 42. Vaeth, M., Kahlfuss, S. & Feske, S. CRAC Channels and Calcium Signaling in T Cell-
909 Mediated Immunity. *Trends Immunol*. **41**, 878-901 (2020).
910 43. Clipstone, N.A. & Crabtree, G.R. Identification of calcineurin as a key signalling enzyme
911 in T-lymphocyte activation. *Nature*. **357**, 695-697 (1992).
912 44. Chen, L. et al. Structure of the DNA-binding domains from NFAT, Fos and Jun bound
913 specifically to DNA. *Nature*. **392**, 42-48 (1998).
914 45. Macián, F., García-Rodríguez, C. & Rao, A. Gene expression elicited by NFAT in the
915 presence or absence of cooperative recruitment of Fos and Jun. *EMBO J*. **19**, 4783-4795
916 (2000).
917 46. Eferl, R & Wagner, E.F. AP-1: a double-edged sword in tumorigenesis. *Nature Reviews*
918 *Cancer*. **3**, 859-868 (2003).
919 47. Marusina, A.I et al. Regulation of human DAP10 gene expression in NK and T cells by Ap-
920 1 transcription factors. *J Immunol*. **180**, 409-417 (2008).
921 48. Azzi, J.R., Sayegh, M.H. & Mallat, S.G. Calcineurin inhibitors: 40 years later, can't live
922 without. *J Immunol*. **191**, 5785-5791 (2013).
923 49. Lee, H.G. et al. Pathogenic function of bystander-activated memory-like CD4(+) T cells in
924 autoimmune encephalomyelitis. *Nat Commun*. **10**, 709 (2019).
925 50. Langmead, B. & Salzberg, S.L. Fast gapped-read alignment with Bowtie 2. *Nat Methods*.
926 **9**, 357-359 (2012).
927 51. Love, M.I., Huber, W. & Anders, S. Moderated estimation of fold change and dispersion
928 for RNA-seq data with DESeq2. *Genome Biol*. **15**, 550 (2014).

929 52. Ritchie, M.E. et al. limma powers differential expression analyses for RNA-sequencing
930 and microarray studies. *Nucleic Acids Res*. **43**, e47 (2015).
931 53. Giles, J.R. et al. Human epigenetic and transcriptional T cell differentiation atlas for
932 identifying functional T cell-specific enhancers. *Immunity*. **55**, 557-574 (2022).
933 54. Yukawa, M. et al. AP-1 activity induced by co-stimulation is required for chromatin
934 opening during T cell activation. *J Exp Med.* **217**, e20182009 (2019).
935 55. Stuart, T. et al. Comprehensive Integration of Single-Cell Data. *Cell*. **177**, 1888-1902
936 e1821 (2019).
937 56. Durinck, S., Spellman, P.T., Birney, E. & Huber, W. Mapping identifiers for the integration
938 of genomic datasets with the R/Bioconductor package biomaRt. *Nat Protoc*. **4**,
939 1184-1191 (2009).